Volume 6, Issue 10 – January – June – 2019

ECORFAN

Journal-Bolivia

ISSN-On line: 2410-4191

10th ANNIVERSARY ECORFAN Special Edition

ECORFAN Journal-Bolivia, Volume 6, Issue 10, January - June 2019, is a journal edited four-monthly by ECORFAN-Bolivia. 21 Santa Lucía, CP-5220. Libertadores – Sucre – Bolivia. WEB: www.ecorfan.org, revista@ecorfan.org. Chief Editor IGLESIAS-SUAREZ, Fernando. MsC. ISSN-On line: 2410-4191. Responsible for the latest update of this number ECORFAN Computer Unit. ESCAMILLA-BOUCHÁN, Imelda. PhD, LUNA SOTO-Vladimir. PhD. 21 Santa Lucía, CP-5220. Libertadores – Sucre – Bolivia, last updated June 30, 2019.

ECORFAN-Journal Bolivia

Definition of the Journal

Scientific Objectives

Support the international scientific community in its written production Science, Technology and Innovation in the Field of Medicine and Health Sciences, in Subdisciplines Engineering, Chemical, Optical, Resources, Food technology, Anatomy, Nutrition.

ECORFAN-Mexico SC is a Scientific and Technological Company in contribution to the Human Resource training focused on the continuity in the critical analysis of International Research and is attached to CONACYT-RENIECYT number 1702902, its commitment is to disseminate research and contributions of the International Scientific Community, academic institutions, agencies and entities of the public and private sectors and contribute to the linking of researchers who carry out scientific activities, technological developments and training of specialized human resources with governments, companies and social organizations.

Encourage the interlocution of the International Scientific Community with other Study Centers in Mexico and abroad and promote a wide incorporation of academics, specialists and researchers to the publication in Science Structures of Autonomous Universities - State Public Universities - Federal IES - Polytechnic Universities - Technological Universities - Federal Technological Institutes - Normal Schools - Decentralized Technological Institutes - Intercultural Universities - S & T Councils - CONACYT Research Centers.

Scope, Coverage and Audience

ECORFAN -Journal Bolivia is a Journal edited by ECORFAN-Mexico S.C in its Holding with repository in Bolivia, is a scientific publication arbitrated and indexed with semester periods. It supports a wide range of contents that are evaluated by academic peers by the Double-Blind method, around subjects related to the theory and practice of Engineering, Chemical, Optical, Resources, Food technology, Anatomy, Nutrition with diverse approaches and perspectives , That contribute to the diffusion of the development of Science Technology and Innovation that allow the arguments related to the decision making and influence in the formulation of international policies in the Field of Medicine and Health Sciences. The editorial horizon of ECORFAN-Mexico® extends beyond the academy and integrates other segments of research and analysis outside the scope, as long as they meet the requirements of rigorous argumentative and scientific, as well as addressing issues of general and current interest of the International Scientific Society.

Arbitration Committee

Assignment of Rights

The sending of an Article to ECORFAN -Journal Bolivia emanates the commitment of the author not to submit it simultaneously to the consideration of other series publications for it must complement the Originality Format for its Article.

The authors sign the Authorization Format for their Article to be disseminated by means that ECORFAN-Mexico, S.C. In its Holding Bolivia considers pertinent for disclosure and diffusion of its Article its Rights of Work.

Declaration of Authorship

Indicate the Name of Author and Coauthors at most in the participation of the Article and indicate in extensive the Institutional Affiliation indicating the Department.

Identify the Name of Author and Coauthors at most with the CVU Scholarship Number-PNPC or SNI-CONACYT- Indicating the Researcher Level and their Google Scholar Profile to verify their Citation Level and H index.

Identify the Name of Author and Coauthors at most in the Science and Technology Profiles widely accepted by the International Scientific Community ORC ID - Researcher ID Thomson - arXiv Author ID - PubMed Author ID - Open ID respectively.

Indicate the contact for correspondence to the Author (Mail and Telephone) and indicate the Researcher who contributes as the first Author of the Article.

Plagiarism Detection

All Articles will be tested by plagiarism software PLAGSCAN if a plagiarism level is detected Positive will not be sent to arbitration and will be rescinded of the reception of the Article notifying the Authors responsible, claiming that academic plagiarism is criminalized in the Penal Code.

Arbitration Process

All Articles will be evaluated by academic peers by the Double Blind method, the Arbitration Approval is a requirement for the Editorial Board to make a final decision that will be final in all cases. MARVID® is a derivative brand of ECORFAN® specialized in providing the expert evaluators all of them with Doctorate degree and distinction of International Researchers in the respective Councils of Science and Technology the counterpart of CONACYT for the chapters of America-Europe-Asia- Africa and Oceania. The identification of the authorship should only appear on a first removable page, in order to ensure that the Arbitration process is anonymous and covers the following stages: Identification of the Journal with its author occupation rate - Identification of Authors and Coauthors - Detection of plagiarism PLAGSCAN - Review of Formats of Authorization and Originality-Allocation to the Editorial Board-Allocation of the pair of Expert Arbitrators-Notification of Arbitration -Declaration of observations to the Author-Verification of Article Modified for Editing-Publication.

Instructions for Scientific, Technological and Innovation Publication

Knowledge Area

The works must be unpublished and refer to topics of Engineering, Chemical, Optical, Resources, Food technology, Anatomy, Nutrition and other topics related to Medicine and Health Sciences.

Presentation of the Content

In the first chapter we present, *Effect of the operating conditions on the particle size distribution by the suspension polymerization process*, by RODRÍGUEZ-PIZANO, José Josué, GRANADOS-RIVERA, Laura Edith, HERNÁNDEZ-ESCOTO, Héctor and CONTRERAS-LÓPEZ, David, with ascription in the Universidad de Guanajuato, as a second article we present, *Graphene oxide used for detection devices of artificial sweeteners not regulated in the food industry*, by GALINDO-GONZÁLEZ, Rosario, ULLOA-VAZQUEZ, Talina, HERRASTI, Pilar, FUENTES-RAMÍREZ, Rosalba, ascription in the Universidad de Guanajuato, Autonomus University of Madrid and CONACYT cathedra in Universidad de Guanajuato , as the following article we present, *Influence of NaCl on the polymerization of vinyl monomers by the suspension process*, by MONTERO, Erika, CONTRERAS-LOPEZ, David, FUENTES, Rosalba and GALINDO, María Del Rosario, with affiliation at the Universidad de Guanajuato, as next article we present, *Nanocristal and ferrite numerical comparison for high frequency and low power electronic converters*, by CASTILLO, Ibsan, PEREZ, Francisco, RODRIGUEZ, Martin, CAMINO, Pedro and FRANCO, Carlos, with affiliation at the Celaya Insitute of Technology.

Content

Article **ECORFAN-Journal Bolivia**
June 2019 Vol.6 No.10 1-12

Effect of the operating conditions on the particle size distribution by the suspension polymerization process

Efecto de las condiciones de funcionamiento en la distribución del tamaño de partícula por el proceso de polimerización en suspensión

RODRÍGUEZ-PIZANO, José Josué†, GRANADOS-RIVERA, Laura Edith, HERNÁNDEZ-ESCOTO, Héctor and CONTRERAS-LÓPEZ, David*

Universidad de Guanajuato. Depto. de Ingeniería Química, División de Ciencias Naturales y Exactas. Noria Alta S/N, Guanajuato, Gto. México 36050

ID 1st Author: *José Josué, Rodríguez-Pizano* / **ORC ID:** 0000-0002-8204-1281**, CVU CONACYT ID:** 887231

ID 1st Coauthor: *Laura Edith, Granados-Rivera* / **ORC ID:** 0000-0002-0863-4230, **CVU CONACYT ID:** 867252

ID 2nd Coauthor: *Héctor, Hernández-Escoto* / **ORC ID:** 0000-0002-0576-0346

ID 3rd Coauthor: *David, Contreras-López* / **ORC ID:** 0000-0003-1384-4766

DOI: 10.35429/EJB.2019.10.6.1.12 Received January 28, 2019; Accepted March 30, 2019

Abstract

In this research, we focus on the study of the operating conditions that influence on suspension process for obtaining (co)polymers of styrene with polar monomers (copolymers of styrene with acrylate of butyl (S-BA) and copolymers of styrene with vinyl acetate (S-VAc)) using the technique of conventional free radical polymerization (FRP). At higher agitation speed, the reaction performance decreases. Likewise, the influence of the molecular weight of the dispersing agent, in this case polyvinyl alcohol (PVA), influences the polymerization performance was also observed. That is, at a higher molecular weight of PVAs, there is an increase in the particle size of the bead and in the polymerization yield. Finally, there is an influence of the polar part on the copolymer both for the yield and for the particle size of the bead. When obtaining copolymers of S-VAc, the yield is lower compared to the respective styrene homopolymer and higher in the S-BA.

Styrene, Suspension, Polar Monomer, Copolymerization, PVA

Resumen

En esta investigación, nos centramos en el estudio de las condiciones operativas que influyen en el proceso de suspensión para obtener (co) polímeros de estireno con monómeros polares (copolímeros de estireno con acrilato de butilo (S-BA) y copolímeros de estireno con acetato de vinilo (S-VAc) utilizando la técnica de polimerización por radicales libres (FRP) convencional. A mayor velocidad de agitación, el rendimiento de la reacción disminuye. Asimismo, la influencia del peso molecular del agente dispersante, en este caso el alcohol polivinílico (PVA), también influye en el rendimiento de la polimerización. Es decir, a un peso molecular más alto de los PVA, hay un aumento en el tamaño de partícula de la perla y en el rendimiento de polimerización. Finalmente, existe una influencia de la parte polar en el copolímero tanto para el rendimiento como para el tamaño de partícula de la perla. Cuando se obtienen copolímeros de S-VAc, el rendimiento es menor en comparación con el homopolímero de estireno respectivo y mayor en el S-BA.

Estireno, Suspensión, Monómero Polar, Copolimerización, PVA

Citation: RODRÍGUEZ-PIZANO, José Josué, GRANADOS-RIVERA, Laura Edith, HERNÁNDEZ-ESCOTO, Héctor and CONTRERAS-LÓPEZ, David. Effect of the operating conditions on the particle size distribution by the suspension polymerization process. ECORFAN Journal-Bolivia. 2019. 6-10: 1-12.

* Correspondence to Author (email: david.contreras@ugto.mx)
† Researcher contributing first author.

1. Introduction

Currently, the polymers area is one of the fastest growing due to the demand of its products in the international market, for this reason this sector needs to invest in research and technology to improve its products or processes to get this type of materials. Polymers have brought great advantages with respect to traditional materials and for their various applications can be used in many sectors of the processing industry. Therefore, they have great versatility and this can be seen in the great development scientific and technological that has allowed the acquisition of new types of materials.[1]

As an example, the preparation of the styrene-maleic anhydride copolymer can be mentioned, which is of great value because it is widely used as a compatibilizing agent in polymer blends and among other uses.[2-4] Such a copolymer system is generally prepared by conventional free radicals. (FRP) and has the characteristic of presenting broad molecular weight distributions (Đ)~2.4. For this reason, suspension polymerization is widely used in the industry to produce high added value particulate products as separation media for chromatography columns, ion exchange resins and supports for immobilization of enzymes, among other uses.[5]

2. Background

The importance of the particle morphology of the polymer (particle size, shape and internal structure) affects the performance of the resin in many important applications and consequently the economic value of the polymeric resin. The morphology of the particles of a polymer resin is often a key quality parameter that must be controlled. Normally, large particles with a relatively uniform size are more desirable. The fine particles can give rise to problems of dust formation, both during handling and bulk processing, also this be a cause of uneven absorption of plasticizers during dry mixing. On the other hand, coarse particles can lead to flow problems during processing and can be a cause for the appearance of fish eyes in the finished product. Finally, large resin particles sometimes do not completely melt during processing, which can significantly impair the appearance and physical properties of the finished articles.

A typical suspension polymerization system is characterized using initiators and monomers that are relatively insoluble in water (this is called continuous phase) and by the fact that the monomer drops are dispersed with aid of a vigorous agitation and small amounts of suspending agents (stabilizers or dispersants). The suspension agents usually used in the process can be of two groups: inorganic compounds insoluble in water such as tricalcium phosphate or water-soluble polymers such as hydroxyethylcellulose or polyvinyl alcohol (PVA).

Several studies [6-10] have established that the stabilizing properties of PVA during the suspension process are dependent on the concentration, degree of hydrolysis and molecular weight. The suspension process is constituted by the continuous phase that represents most of the reaction medium, where the suspension agent is solubilized and combined with the speed of agitation, it avoids that coalescence does not occur in the dispersed phase as well as control the final particle size of the polymer. The dispersed phase is formed by the monomer and the initiator. The operating conditions that must be taken care of are the reaction temperature, the speed of agitation and the concentration of the dispersing agent in the medium.[8, 11] At the end of the polymerization, pearls are obtained so that their purification process and separation is relatively simple. Thus, the use of the dispersing agent (or suspending agent) is the crucial ingredient for carrying out said polymerization process.

It has been found that at lower molecular weights of the PVA, more stable suspensions are produced than with those of high molecular weight and generating larger particle sizes. With the use of a high molecular weight of PVA have been obtained sizes well-defined particles. It should be noted that the initiator begins inside the drops to initiate the polymerization process. The interaction between the macroradicals is strong enough to facilitate the aggregation of the monomer units. In addition to the growth of the aggregates, it also proceeds by coalescence, forming primary particles that are responsible for the porosity of the formed grains.[12,13]

ISSN-On line 2410-4191

RODRÍGUEZ-PIZANO, José Josué, GRANADOS-RIVERA, Laura Edith, HERNÁNDEZ-ESCOTO, Héctor and CONTRERAS-LÓPEZ, David. Effect of the operating conditions on the particle size distribution by the suspension polymerization process. ECORFAN Journal-Bolivia. 2019.

Various reports have been published about the effects of polymerization conditions such as the speed of agitation, type and concentration of the suspending agent, the monomer-water volume ratio, monomer reflux conditions, temperature and conversion.[14-16] Although the suspension process has been extensively studied, its understanding is still limited. There is a large amount of experimental effort and empirical knowledge to design new resins. The less advanced issues are related to the rheological behavior of the reaction mixture during polymerization and the phenomena of coalescence that determine the particle size distribution in this last stay.13 Obtaining a well-defined size and particle size distribution (PSD) are subject to intensive research for many suspension polymerization processes.[17]

Approximately 80% of the commercial production of PS and its copolymers is by the process of suspension polymerization.[5] This material is mainly used for packaging and production of disposable materials, due to its low cost and good processing capacity; the most used form is the expanded one because it is highly required in disposable and construction products, thermal insulators and in the protection of objects packaging.18 The present research is focused on studying some characteristics of the suspension process to carry out the synthesis of styrene copolymers with polar vinyl monomers such as vinyl acetate (VAc) and butyl acrylate (BA). The reason is that within the industrial sphere, this process is still maintained with a trial-and-error approach with few scientific bases, generating negative repercussions economically.8

The spirit of our study is focused to increasing the knowledge of the factors that govern the polymerization of styrene with polar monomers by the process of suspension to create more advanced and controlled structures, given that this is a part of a project in which some techniques of controlled free radical polymerization (CRP) will be used, in particular nitroxide-mediated polymerization (NMP) and reversible addition-fragmentation chain transfer process (RAFT). Likewise, the intention of obtaining this type of copolymers is to use them as support materials or compatibilizers in mixtures of conductive polymers within the assembly of a solar cell for example.

However, the effectiveness of such applications requires a priori knowledge of the operating conditions and their characteristics of the suspension process of conventional free radical polymerizations and subsequently transfer them to CRP.[19]

Today, our work of group is focused on this type of synthesis approach by mechanical agitation. Therefore, the objectives of this investigation are: 1. To find which are the operating conditions that obey the suspension process via magnetic stirring, 2. To control the particle size and distribution of the pearls that are formed and 3. To study the statistical behavior that is focused on said study. All this, accompanying the objectives the analysis by IR-FT, NMR and viscosimetry of solutions.

3. Materials and Methodology

Styrene, butyl acrylate, vinyl acetate and benzoyl peroxide (BPO) were of analytical grade (Sigma-Aldrich), the monomers were previously washed to remove the inhibitor by conventional methods. The ethanol was of RA grade. Different molecular weights and degree of hydrolysis of PVA were used as specified by the supplier (see **Table 1**, Sigma-Aldrich). The experiments of the suspension were carried out in a 250 mL reactor and the stirring was by magnetic agitation.

The continuous and dispersed liquid phases were prepared as shown in **Table 1**. In the batch suspension polymerization experiments, we investigated the effect of three variables: agitation speed to the reaction system, concentration and molecular weight of the suspension on the conversion profiles, on the molecular weight of the polymeric material obtained, size and distribution of the particle size derived from the suspension process. The experiments were carried out for the homopolymerization of styrene and two copolymerizations of S-BA and S-VAc.

ISSN-On line 2410-4191

Polyalcohol	Molecular weight (Da)	Degree of hydrolysis
PVA1	13 000 – 24 000	87 – 90 %
PVA2	30 000 – 70 000	87 – 90 %
PVA3	89 000 – 98 000	87 – 90 %
PVA4	124 000 – 130 000	87 – 90 %
Continuous phase:	Distilled water (100 mL) + Stabilizer (PVA)	
Dispersed phase:	Monomer(s) + initiator (BPO) Initiator concentration: 12.1 g/L=0.05 mol/L	

Table 1 Agents of dispersion and properties of liquids in the two phases in the initial stage of polymerization (85 °C)

The average molecular weights were determined with a Cannon-Fenske #25 viscometer and the Mark-Houwink equation. The Mark-Houwink constants for the systems used are presented in **Table 2**, the percentage is indicated by weight with respect to polar monomer. The PVA solutions were prepared by dissolving the polyvinyl alcohol in water at temperature between 60 and 75 °C. The solutions were kept in agitation until they presented a transparency, so they were filtered and stored before use (for not more than a week).

Polymer [a]	α^b	$Kx10^3$ [b] (cm^3/g)
S	0.530	37.0
S-VAc 10%	0.530	37.7
S-VAc 5%	0.530	40.6
S-VAc 1%	0.530	44.1
S-AB 10%	0.552	34.0
S-AB 5%	0.541	35.5
S-AB 1%	0.531	36.7

Table 2 Mark-Houwink Constants[20]

a BA: Butyl acrylate; S: Styrene; VAc: Vinyl acetate.

b Referred to 25 ° C and dissolved in toluene.

Conversion profiles. The monomer conversion was calculated by gravimetric analysis of samples taken from the reactor at sampling times chosen by means pipettes (0.8 mm D.I.) and placed on aluminum plates containing an inhibitor solution (hydroquinone).

Towards the end of the reactions, the representative sampling of the particles in suspension became more difficult; despite the agitation in the reactor, the polymer particles tended to settle to the bottom of the reactor because the density of the formed material is significantly higher than that of the water (ρ_{PS}=1.04 g/cm^3).

3.1. Synthesis of styrene homopolymer

A typical procedure for the homopolymerization of styrene to conventional free radicals (FRP) by means the suspension process was carried out using PVA as the dispersing agent. In the dispersed phase, 18,180 g of styrene (175 mmol) and 0.242 g of benzoyl peroxide (BPO, 0.1 mmol) were added, therefore there is a molar ratio of monomer: initiator of 1750: 1. The synthesis was carried out in a 250 mL Batch reactor, using 100 mL of distilled water as a continuous phase (in that phase the PVA was already dissolved, two concentrations of 5 and 10 g / L were used), the speed of agitation of the system (three agitation speeds, 300, 500 and 800 rpm were used) at a temperature of 85±2 °C until an approximate yield of 80% was obtained. For the purification of the polymer, we proceeded with filtration by gravity and washed with ethanol (2 times) to remove the remaining PVA on the surface of the beads. It got dry at room temperature until a constant weight was obtained. It was sent to characterize by NMR ^{1}H, IR-FT, viscosimetry and sieving to obtain the particle size.

The determination of the NMR ^{1}H spectra was carried out in a Bruker Ascend 400 MHz equipment of 7.07 Teslas of magnetic field intensity in tubes of 5 mm external diameter, using deuterated chloroform ($CDCl_3$) at room temperature. It worked 16 scans with samples of 25 mg in 0.6 mL of the deuterated solvent. The chemical shifts (δ) were measured in parts per million (ppm). Tetramethylsilane (TMS) was used as internal reference for the NMR spectra. To obtain the spectra of FT-IR was in a Perkin-Elmer Spectrum 100 equipment. The samples were analyzed in tablet form by means of a mixture with KBr. The working frequency range was 4000-400 cm^{-1} using 32 scans and 4 cm^{-1} resolution. By means of this technique the absorption bands present in the various polymeric compounds obtained were analyzed.

ISSN-On line 2410-4191

3.2. Synthesis of styrene copolymers

The copolymerization of the styrene was carried out according to the procedure described: "*Synthesis of styrene homopolymer*" with the difference that the concentration of the polar monomer (butyl acrylate (BA) or vinyl acetate (VAc)) was varied in 10%, 5% and 1% by weight with respect to styrene added to the system, the free radical initiator was used BPO to maintain a molar ratio of 1750: 1. It should be noted that for the copolymerizations only the PVA3 was used at a concentration of 5 g/L of the dispersing agent.

4. Results and Discussion

4.1. Homopolymerization of styrene

The following results are related to the use of the PVA3 dispersant agent, it has been selected because is this in the middle part of **Table 1**, these results are so similar with those obtained the other dispersing agents. The agitation speed in the reaction medium and the concentration of the dispersing agent are natural variables that can be manipulated to control the morphology of the particles in the suspension polymerization reactors, so it is acceptable that these variables do not cause any influence on the kinetics of the polymerization. **Figure 1A** and **B** show the evolution of monomer conversion (% X) and polymerization rate (R_p=d%*X*/d*t*) for runs performed at different concentrations with PVA3 at 300 rpm and 85 °C. The behavior shown in **Figure 1** is also observed in the case of the agitation speeds of 500 and 800 rpm. It can be seen in **Figure 1A** that there is a retardation effect in the reaction medium due to the presence of the stabilizing agent since we believe that by adding it to the medium, these agents were used as they were provided without any other purification, which could explain why the reaction is delayed although this phenomenon is not important for the purposes established in the present work however some differences can be observed in the range of conversions from 5 to 80% but from the practical point of view the reactions end at a conversion of the monomer in about 85% at 2 h of reaction, except for the case of the lowest concentration (0.01 g/L) which extends until 3 h of reaction.

This can be explained by the fact that the effect of the immiscibility between the two phases governs more because there is practically no formation of pearls and therefore, there is greater freedom in the dispersed medium for the polymerization reaction, resulting in a larger population of monomer present in the medium and avid radical species of these vinyl type molecules.

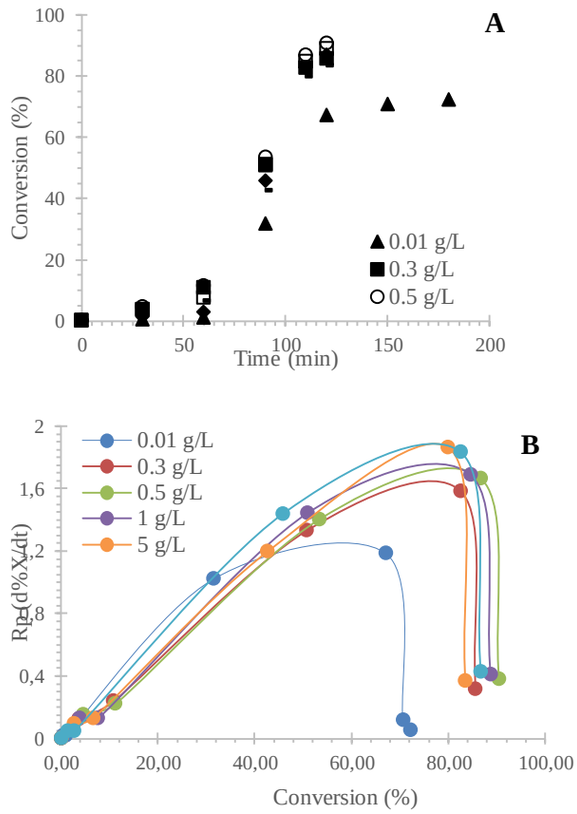

Figure 1 Evolution of monomer conversion (**A**) and polymerization rates (**B**) for the suspension polymerization of styrene at 85 °C and 300 rpm using PVA3

Figure 2 shows the experimental data for the evolution of the average particle size of styrene at different concentrations of PVA3 at the same temperature (85 °C) and at different rates of agitation in the polymerization system. It can be seen that at low concentrations of the suspension agent, the size of the bead is higher than at high concentrations, clearly indicating the low influence of the PVA concentration in the system, which does not have an important participation during the process of pearl formation, governing more the coalescence process and that is according to what is indicated by Lin et al.[16]

ISSN-On line 2410-4191

However, this is not true for high speeds of agitation as it happens at 800 rpm because they govern more the shear forces, allowing the rupture process to be the main phenomenon present in the process.[24]

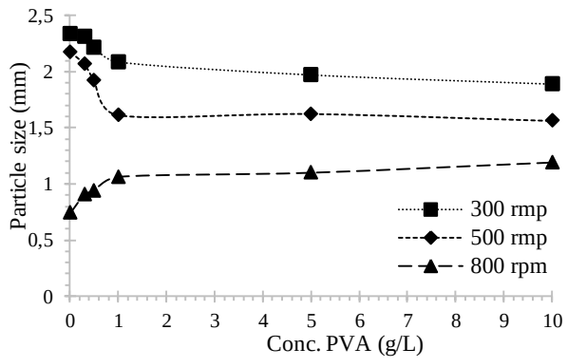

Figure 2 Evolution of the average particle size of polystyrene at different agitation speeds with PVA3

The process of rupture and coalescence comes when the viscosity of the suspended particles is low, and the shearing forces created by the agitation become strong enough to break the particles fused into smaller particles. When the viscosity of the droplets is high such as in the case at moderate to intermediate conversions, the stirring may not be sufficient to interrupt coalesced particles.

In spite this, the protective layer (high coverage) prevents coalescence of the particles in the larger ones and therefore small solid particles will form during the reaction. Only when the concentration of adsorbed polymer segments is not high enough, bridging due to entanglement can be broken by shear forces. In this case the protective layer is not as effective as that of higher concentrations, probably due to the lower density of the polymeric segment and thus coalescence occurs in larger particles. With high molecular weight species, the protective film is thicker than in the case discussed above (due to the much larger molecular weight and size) and therefore coalescence can be effectively prevented even at lower PVA concentrations.[5, 12, 24]

The average particle size and size distribution in suspension polymerization reactors is important for certain applications. Maintaining the average particle size constant during the scaling of the reactor is a challenge in polymer engineering.

The prediction and control of the final particle size distribution is associated with the evolution of the droplet size distribution in the monomer dispersion of the aqueous continuous phase. We can observe this by means of the effect of the concentration of the suspension agent to different speeds on the particle size **(see Figure 2)** and on the size distribution **(see Figure 4)**, showing that a reduction in the concentration of PVA produces a larger particle size and a larger particle distribution size, added to the agitation speed imparted to the system (**see Figure 3**), being the latter an important factor In the dynamic process of coalescence and rupture of the particles in the dispersed medium.

Concluding that, at a higher agitation speed, the average particle size decreases thanks to the effect of the cutting forces that are printed for the formation of the bead.

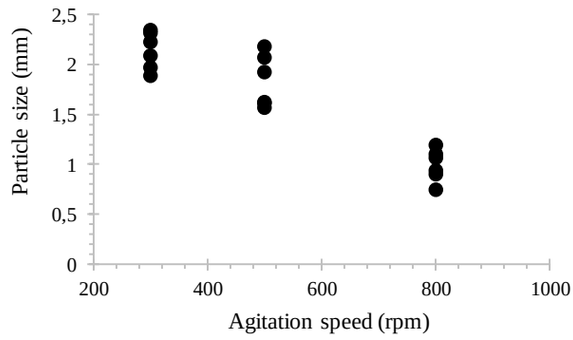

Figure 3 Evolution of the average particle size at different agitation speeds with PVA3

After drying the pearls, the particle size distribution (PSD) was obtained by means of a sieving (standard ASTM sieving method D1291-87) and recording the weight of each size fraction. These results are shown in **Figure 4** corresponding to the agitation speeds and in **Figure 5** can be seen the evolution of the PSD at different concentrations of the PVA3 dispersion agent.

The distribution presents a tendency of decrease of the average diameter when the concentration of the PVA and the speed of agitation increase. This is due to the breaking of the larger particles and the stabilization of the smaller ones as the PVA is added.

ISSN-On line 2410-4191

The effect on the distribution becomes narrower as the agitation speed increases. In the case of the agitation speed of 500 rpm, the distribution is narrower than at 300 rpm and the effect of the PVA is the same resulting in a narrower PSD which is not observed at 800 rpm and is due to the existence of a greater shear force in the system. Therefore, as the stirring speed increases the PSD becomes wider. In other words, while the concentration of the dispersing agent increases the PSD decreases and the average size also decreases.

Figure 4 Representative particle sizes at different agitation speeds with PVA3: **a**) 300 rpm, **b**) 500 rpm, **c**) 800 rpm

According to **Figure 5**, the recurrent modification of the agitation speed and the concentration of the dispersant agent results in a bimodal PSD in the polymerization of the suspension. For purposes of this work, the agitation speed and stabilizer agent concentrations are of interest to observe the change of the final particle size of the polymer, without the need to introduce additional changes in other variables of the reaction conditions of the polymerization or the suspension process itself.

It should be noted that the concentration of 0.01 g/L of PVA maintains an erratic behavior during the stabilization process of the suspension and although the amount of the dispersing agent in the system is small, it can be observed that it is sufficient to affect the polymerization process.

This phenomenon can be clearly seen in **Figure 5c**. At low concentrations of PVA, the surface coverage on the particle is poor and therefore the coalescence will occur when it is in contact with other particles.

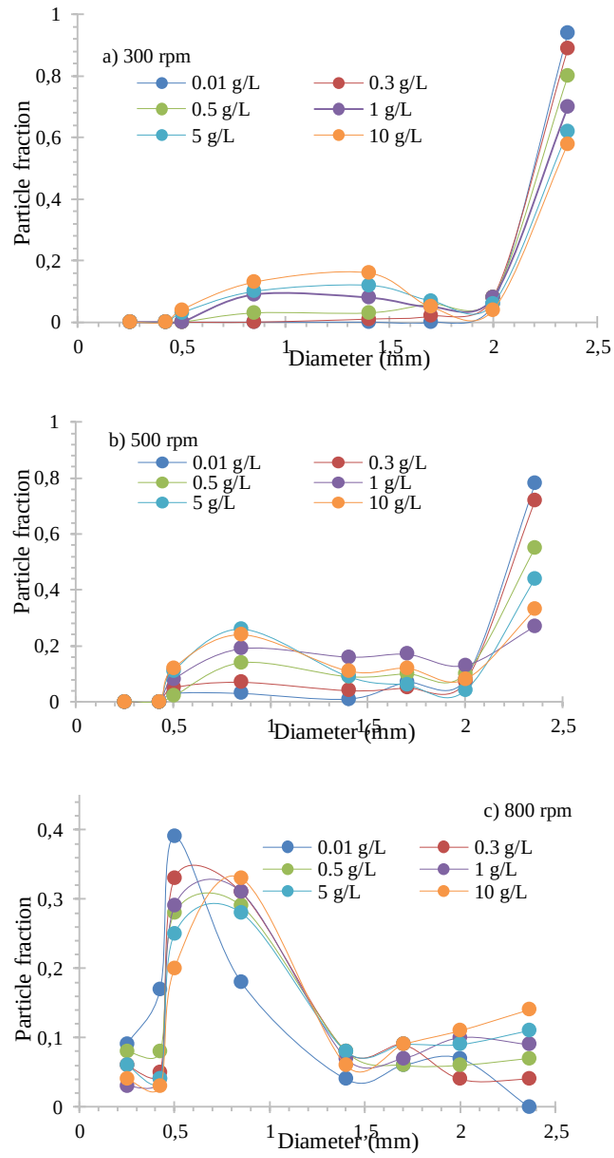

Figure 5 Particle size distribution at different agitation speeds with PVA3, **A**) 300 rpm, **B**) 500 rpm and **C**) 800 rpm

The influence that the molecular weight of the dispersing agent has on the size of the particle (bead) in the polymerization of styrene can be observed in **Figure 6**. The size of the bead has a slight increase and as the speed of agitation decreases, the particle size tends to increase. Therefore, there is a certain trend with the size in relation to the agitation speed since at 300 rpm an average particle size of 2.14 millimeters is obtained, at 500 rpm there is a size of 1.83 millimeters and at 800 rpm a size of 0.99 millimeters. The average size shows a slight tendency to decrease in diameter when the molecular weight of the PVA decreases and this is due to the rupture of the larger particles and to the stabilization of the smaller ones as the dispersing agent is added.

ISSN-On line 2410-4191

The results of the suspension polymerization show that the low molecular weight suspension agents (PVA1 and PVA2) are better stabilizers than those of high molecular weight, due to an ageing phenomenon that is related to the formation of a rigid film in liquid-liquid interface.

It has been documented that this phenomenon of ageing decreases with the increase in molecular weight and the degree of hydrolysis that the dispersant has.[24, 25] However, in cases where it is carried out with high molecular weight suspension agents (PVA3 and PVA4), there is a more definite pearl production.

This is due to the agglomeration of particles that are produced with PVA. The thickness of the polymer adsorption layer increases with the increase in molecular weight and with the increase in particle size.[26]

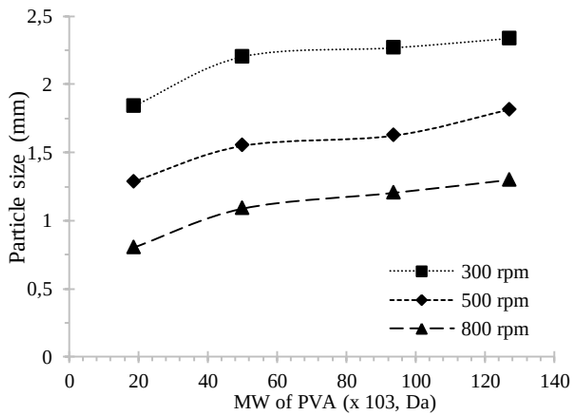

Figure 6 Influence of PVA MW on particle size at different agitation speeds

The influence of molecular weight of the dispersing agent on the molecular weight of the obtained polymer can be seen in **Figure 7**, this behavior exhibits a proportional increase with the size of the main chain of the PVA and this confirms what was observed in **Figure 6** with respect to the agglomeration of the low molecular weight suspension agents and the process of the size of the suspended particle, thickness of the adsorbed layer and physical properties of the reaction of the monomer and polymer.

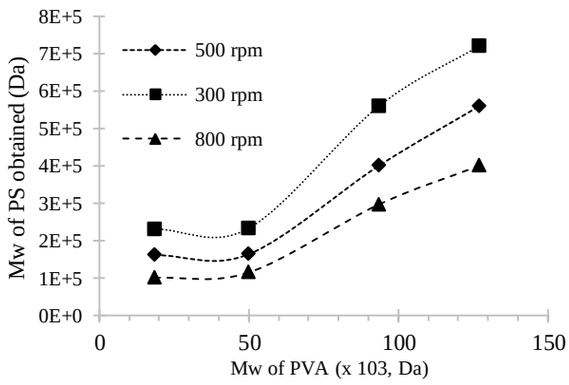

Figure 7 Influence of the molecular weight of the PVA on the molecular weight of the polystyrene obtained at different agitation speeds

It can be seen in Figure 8 the yields of homopolymerization of the styrene with PVA2 and PVA3 at different concentrations (5 and 10 g/L) and agitation speeds (300, 500 and 800 rpm) at 85 ± 2 °C. According to this, it is obtained a higher yield in the three agitation speeds when a concentration of 5 G/L is used with any of the dispersing agents, compared with the systems in which it is worked with a concentration of 10 g/L. This behavior is due to the above described in relation to the coverage of the dispersing agent on the surface of the polymer particle, being low and the coalescence occurs in contact with other particles. Added to that there is a greater space to obtain more freedom during the polymerization process.

Therefore, there is a high probability that the vinyl molecules can be polymerized by the phenomenon of avidity of consumption of the monomers. It is noted that when we used the PVA3, there is a higher performance than when using the PVA2. As already discussed, it is due to both the size and the mobility of the polymer chain of the dispersing agent, so PVA2 maintains a greater proportion of available hydrogen bridges with the continuous phase, which leads to having a lower yield of the polymer formed.

ISSN-On line 2410-4191

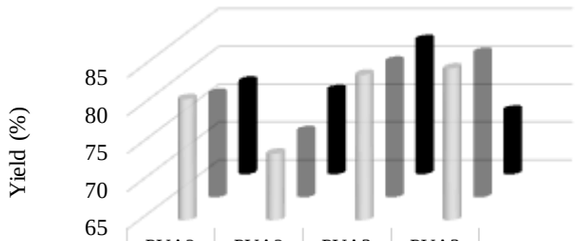

	PVA2 (5 g/L)	PVA2 (10 g/L)	PVA3 (5 g/L)	PVA3 (10 g/L)
300 rpm	80,95	73,77	84,17	86,98
500 rpm	78,61	73,71	82,88	84,02
800 rpm	77,2	76,08	82,69	73,38

Figure 8 Performance of styrene homopolymers at different agitation speeds by the suspension process. The parentheses indicate the concentration of the dispersing agent

4.2. Copolymerization with Vinyl Acetate

According to what was observed during the styrene homopolymerization process, there are copolymerization similar behaviors, so that only the results obtained for the styrene-vinyl acetate copolymers (S-VAc) and for the styrene-butyl acrylate system (S-BA) focused on the yields at different concentrations of the polar comonomer (10, 5 and 1% by weight in the feed in relation to styrene). We work with PVA2 and PVA3 along with what has already been discussed because they are the ones that present satisfactory results during the suspension process in polymerization.

For the S-VAc system, it is observed in **Figure 9** the yields obtained at different concentrations of vinyl acetate to form the corresponding copolymer, identifying that at the concentration of 1% by weight of the polar monomer in 10 and 5 g/L of the PVA3 lower yields are obtained comparing with the corresponding result of the homopolymerization of the styrene, otherwise with the use of the PVA2 at a concentration of 10 g/L.

This is to the affinity that exists between polyvinyl acetate and PVA, due to its physicochemical characteristics, which may be forming some type of intermolecular bonds such as hydrogen bridges mainly with the low molecular weight dispersion agent. Finally, there are better yields of the polymerization process with the use of PVA2 than with PVA3.

From the point of view of the reactivity ratios to the S-VAc system (r_1=57.8, r_2=0.08),[20] it indicates that polystyrene type radicals react with vinyl acetate at a speed close to 0.02 which can react with the styrene itself if both monomers are present at the same concentration. A similar interpretation can be made with the radicals derived from the VAc, which indicates that it reacts with styrene at a rate of 12.5 times that with vinyl acetate at the same concentration. This allows us to explain that there are lower yields compared with the homopolymerization of styrene. It should be noted that since r_1 is much larger than r_2, the copolymer formed contains long sequences of styrene units interspersed with occasional units of vinyl acetate generating a copolymer with a random tendency.[27]

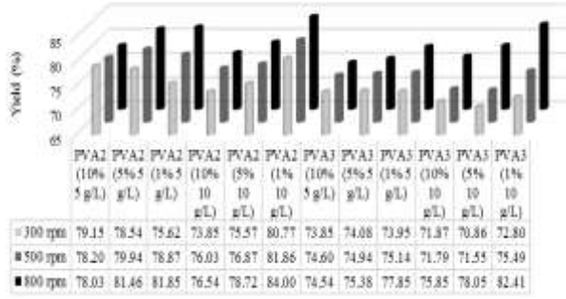

	PVA2 (10% 5 g/L)	PVA2 (5% 5 g/L)	PVA2 (1% 5 g/L)	PVA2 (10% 10 g/L)	PVA2 (5% 10 g/L)	PVA2 (1% 10 g/L)	PVA3 (10% 5 g/L)	PVA3 (5% 5 g/L)	PVA3 (1% 5 g/L)	PVA3 (10% 10 g/L)	PVA3 (5% 10 g/L)	PVA3 (1% 10 g/L)
300 rpm	79.15	78.54	75.62	73.85	75.57	80.77	73.85	74.08	73.95	71.87	70.86	72.80
500 rpm	78.20	79.94	78.87	76.03	76.87	81.86	74.60	74.94	75.14	71.79	71.55	75.49
800 rpm	78.03	81.46	81.85	76.54	78.72	84.00	74.54	75.38	77.85	75.85	78.05	82.41

Figure 9 Yield of styrene-vinyl acetate copolymers using PVA2 and PVA3

With respect to the FT-IR spectrum of the (co) polymer S-VAc at 10% by weight in the feed with respect to styrene and obtained by the suspension process using the PVA3. It was analyzed qualitatively, and its corresponding bands can be observed in **Figure 10**, the copolymer exhibits the same characteristic absorption bands shown by the homopolymer units.

In this spectrum, a band is shown in 2915 cm^{-1} representing the vibration of CH from the methyl, methylene and methine that are present in the main chain of the polymer, the bands in 1941, 1878 and 1804 cm^{-1} correspond to a monosubstitution in the aromatic ring belonging to the unit of styrene, in the same way we can observe a signal in 1723 cm^{-1}, characteristic of the elongation type vibration of a carbonyl group that corresponds to the acetate group.

ISSN-On line 2410-4191

The signal at 1598 cm^{-1} represents the elongation vibration of a CC double bond of aliphatic type, as we observe in 1487, 1454 and 1373 cm^{-1} represent the deformation vibration of a CH bond of methyl, methylene and methine groups, the band that confirms the existence of a CO bond is at 1269 cm^{-1}.

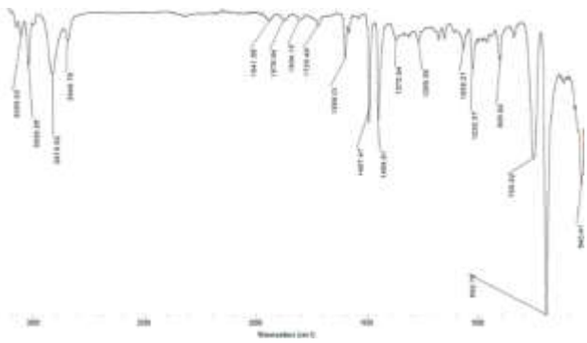

Figure 10: IR-FT spectrum of the 10% styrene-vinyl acetate copolymer in the feed

In **Figure 11** (as in the case of the FT-IR, a comparison was made with the homopolymer of styrene), in the region between 0.8 to 1.0 ppm are the contributing signals of the VAc in the copolymer corresponding to methyl, also observed that in 1.2 to 2.0 ppm are the protons that are due to the methylene and methine that make up the main chain of the polymer and a group in 2.05 and 2.2 ppm that are due to the methine (-CH-) that bound the ester group of the acetate . With respect to the contribution of styrene, the signals in the region of 6.3 to 7.1 ppm are due to the aromatic protons.

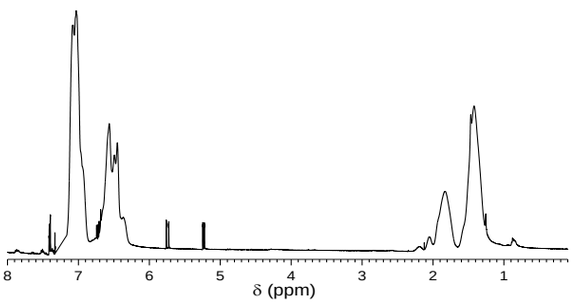

Figure 11 RMN ^{1}H spectrum of styrene-vinyl acetate copolymer at 10% in the feed with respect to styrene

4.3. Copolymerization with Butyl Acrylate

The yields of copolymers of styrene with butyl acrylate, these can be seen in **Figure 12**. It is generally appreciated that by increasing the concentration of the polar monomer in the medium and the concentration of PVA.

The polymer conversion increases in both cases, this may be due to the interactions exerted by the polar monomer in the reaction medium, the formation of the copolymer is favored when it is in a greater percentage. Although we can notice that using the PVA3 has a higher yield than with the PVA2. This could be related to the configuration that the PVA3 acquires in the reaction medium because it is a larger chain, having a ball configuration and grateful to this, it does not allow it to easily form intermolecular links with the continuous phase as it would be the case of PVA2. The chain of polymer is considerably shorter and can acquire a linear configuration to have a better mobility and form intermolecular bonds with the continuous phase and the polar monomer, decreasing the yield of the obtained polymer.

Now, from the point of view of the reactivity indexes presented by the S-BA system (r_1=0.698, r_2=0.164),[20] it indicates that the polystyrene type radicals react with butyl acrylate at a close speed of 1.43 that you can react with the styrene itself if both monomers are present at the same concentration. A similar interpretation can be made with the radicals derived from BA, which indicates that it reacts with styrene at a rate of 0.03 times that with butyl acrylate at the same concentration. This allows us to explain that there are higher yields compared with the homopolymerization of styrene. It should be noted that since r1 is slightly larger than r2, the copolymer formed contains sequences of styrene units interspersed with butyl acrylate units, generating a copolymer with an alternating tendency.[27]

The FT-IR spectrum of the (co) polymer at 10% by weight in the feed with respect to the styrene obtained by the suspension process using the PVA3, was analyzed qualitatively and its bands can be observed in **Figure 13**, where it was carried out a comparison between these materials. The copolymer exhibits the same characteristic absorption bands shown by the homopolymer units.

ISSN-On line 2410-4191

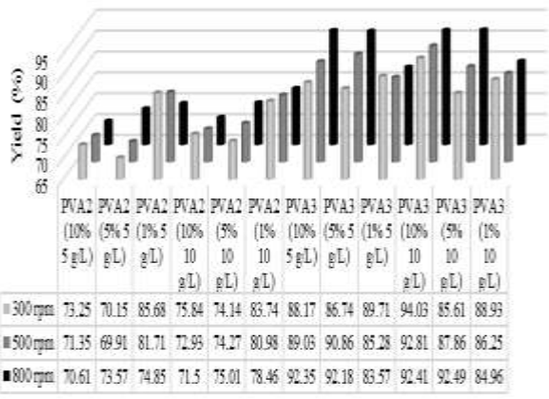

Figure 12 Performance of styrene and butyl acrylate copolymers using PVA2 and PVA3

It can be seen in the FT-IR spectrum of the styrene-vinyl acetate copolymer In this spectrum, a band is shown in 2912 cm^{-1} representing the vibration of CH from the methyl, methylene and methine that are present in the main chain of the polymer, the signals in 1943, 1871 and 1800 cm^{-1} correspond to a monosubstitution in the aromatic ring belonging to the premiere unit, in the same way we can observe a signal in 1725 cm^{-1}.

The characteristic of the vibration of elongation type of a carbonyl group corresponding to the acrylate group.

The signal at 1594 cm^{-1} represents the elongation vibration of a CC double bond of aliphatic type, as we observe in 1492, 1443 and 1375 cm^{-1} represent the deformation vibration of a CH bond of methyl, methylenes and methine groups, the band that confirms the existence of a CO bond is at 1269 cm^{-1}.

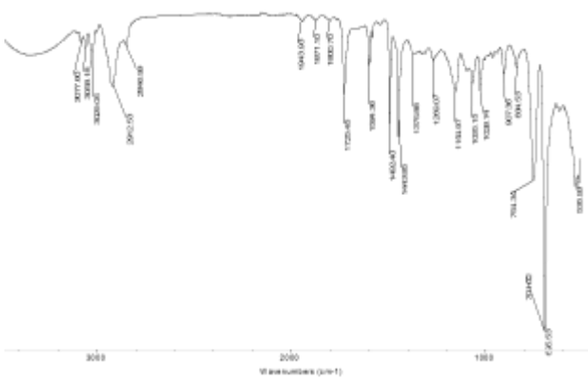

Figure 13 IR-FT spectrum of 10% by weight styrene-acrylate copolymer in the feed

In **Figure 14**, in the region between 0.5 to 0.8 ppm are the contributing signals of the BA in the copolymer corresponding to methyl, it is also observed that in 0.8 to 1.8 ppm are the protons that are due to the methylene and methine that make up the main chain of the polymer and a group in 1.8 and 2.0 ppm that are due to the methine of the main chain (-CH-) that binds the ester group of the acrylate. There is a multiplet corresponding to the methylene (-CH-) of the butyl after the acrylate ester. With respect to the contribution of styrene, the signals in the region of 6.0 to 6.9 ppm are due to the styrene aromatic protons.

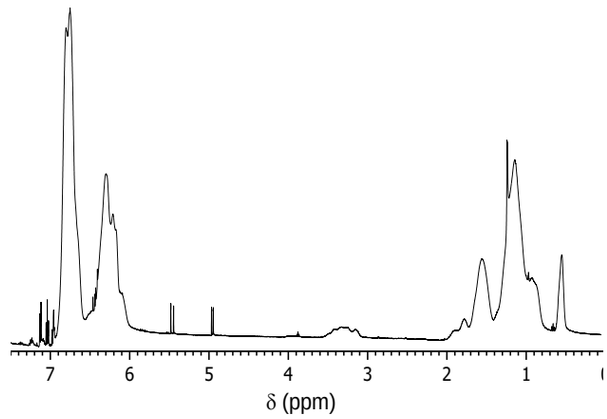

Figure 14 RMN ^{1}H spectrum of styrene-10% butyl acrylate copolymer in the feed

5. Conclusions

According to the observed, it was found that by decreasing the molecular weight and increasing the concentration of the dispersant agent (PVA), there is a lower conversion in the homopolymers of styrene. The influence of the speed of agitation is noticeable when increasing it, as the distribution of particle size is less polydisperse at lower speed.

On the other hand, it was found that by decreasing the concentration of vinyl acetate in the reaction medium, this favors the formation of the corresponding copolymer with a high concentration of dispersant agent.

In the case of styrene and butyl acrylate copolymers, it was found that by increasing the concentration of the polar monomer and the concentration of the dispersing agent, the conversion of the corresponding copolymer is favored.

ISSN-On line 2410-4191

Based on the above, this is a very good approximation to the knowledge of the optimal conditions for obtaining this type of styrene polymers.

6. Acknowledgements

David Contreras-López acknowledges the financial support of this research by PRODEP through the grant for project DSA/103.5/16/10374.

7. References

(1) Utracki LA. Polymer Blends Handbook: Kluwer Academic Pub; **2002**

(2) Wu Y, Zhang H, et al. Journal of Applied Polymer Science. **134**(36), 45281 **(**2017)

(3) Wu S, Wang L, et al. Journal of Applied Polymer Science. **134**(35), 45251 (2017)

(4) Khan DM, Kausar A, et al. Fullerenes, Nanotubes and Carbon Nanostructures. **24**(3),202 (2016)

(5) Ferdinand Rodriguez CC, Christopher K. Ober, Lynden Archer. Principles of Polymer Systems. Sixth Edition ed. USA: CRC Press; **2014**

(6) Ramirez JC, Herrera-Ordonez J, et al. Polymer **47**(10),3336 (2006)

(7) Hong S, Albu R, et al. Polymer International. **55**(12),1426 (2006)

(8) Zhang C, Li X, et al. Journal of Applied Polymer Science. **133**(48), 44270 (2016)

(9) Lu Y, Liu X, et al. Journal of Applied Polymer Science. **134**(32),45111 (2017)

(10) Patnam PL, Ray SS, et al. Journal of Applied Polymer Science. **134**(13), 44645 (2017)

(11) Lenzi MK, Cunningham MF, et al. Journal of Applied Polymer Science.**96**(5), 1950 (2005)

(12) Vivaldo-Lima E, Wood PE, et al. Industrial & Engineering Chemistry Research. **36**(4), 939 (1997)

(13) Dowding PJ, Vincent B. Colloids and Surfaces A: Physicochemical and Engineering Aspects. **161**(2), 259 (2000)

(14) Jalili K, Abbasi F, et al. Journal of Cellular Plastics. **45**(3), 197 (2009)

(15) Castor CA, Sarmoria C, et al. Macromolecular Theory and Simulations. **23**(8), 500 (2014)

(16) Lin W, Biegler LT, et al. Chemical Engineering Science. **65**(15), 4350 (2010)

(17) Kalfas G, Yuan H, et al. Industrial & Engineering Chemistry Research. **32**(9), 1831 (1993)

(18) Ballner D, Herzele S, et al. ACS Applied Materials & Interfaces. **8**(21), 13520 (2016)

(19) Contreras-López D, Albores-Velasco M, et al. Journal of Applied Polymer Science. **134**(29), 45108 (2017)

(20) Brandrup J, Imnergut EH, et al. Polymer Handbook. 4th ed. N. Y., USA: John Wiley & Sons, Inc.; **1999**

(21) Tefera N, Weickert G, et al. Macromolecular Chemistry and Physics. **195**(9), 3067 (1994)

(22) Almog Y, Levy M. Journal of Polymer Science: Polymer Chemistry Edition. **19**(1), 115 (1981)

(23) Regina-Mazzuca AM, Ark WF, et al. Industrial & Engineering Chemistry Product Research and Development **21**(2), 139 (1982)

(24) Konno M, Arai K, et al. Journal of Chemical Engineering of Japan. **15**(2), 131 (1982)

(25) Zhang C, Li X, et al. Journal of Applied Polymer Science. **133**(48), 21544 (2016)

(26) Rodrigo R, Toro CA, et al. Journal of Applied Polymer Science. **124**(2), 1431 (2012)

(27) Hagiopol C. Copolymerization. Toward a systematic approach. New York: Kluwer Academic/Plenum Publisher; **1999**

RODRÍGUEZ-PIZANO, José Josué, GRANADOS-RIVERA, Laura Edith, HERNÁNDEZ-ESCOTO, Héctor and CONTRERAS-LÓPEZ, David. Effect of the operating conditions on the particle size distribution by the suspension polymerization process. ECORFAN Journal-Bolivia. 2019.

Article **ECORFAN-Journal Bolivia**
June 2019 Vol.6 No.10 13-18

Graphene oxide used for detection devices of artificial sweeteners not regulated in the food industry

Óxido de Grafeno empleado en dispositivos de detección de edulcorantes artificiales no regulados en la industria alimenticia

GALINDO-GONZÁLEZ, Rosario[1,3]†*, ULLOA-VAZQUEZ, Talina[1], HERRASTI, Pilar[2], FUENTES-RAMÍREZ, Rosalba[1]

[1]*Universidad de Guanajuato, Natural and Exact Sciences Division, Department of Chemistry Engineering.*
[2]*Autonomus University of Madrid, Department of Applied Physical Chemistry*
[3]*CONACYT cathedra in Universidad de Guanajuato, Natural and Exact Sciences Division*

ID 1st Author: *Rosario, Galindo-González* / **ORC ID:** 0000-0002-3612-1555, **CVU CONACYT ID:** 223987

ID 1st Coauthor: *Talina, Ulloa-Vazquez* / **CVU CONACYT-ID:** 664273

ID 2nd Coauthor: *Pilar, Herrasti* / **ORC ID:** 0000-0003-1067-0780

ID 3rd Coauthor: *Rosalba, Fuentes-Ramírez* / **ORC ID:** 0000-0003-0520-3387, **CVU CONACYT ID:** 202669

DOI: 10.35429/EJB.2019.10.6.13.18 Received: February 28, 2019; Accepted: April 20, 2019

Abstract

In this work, electrochemical sensors were developed for the detection of artificial sweeteners such as D-sorbitol and Maltitol in aqueous solutions. These compounds are classified as polyalcohols and are widely used in the food and beverage industry to replace common sugar. However, their consumption is not currently regulated, and excessive use leads to consequences in the body such as increased blood glucose levels. Graphene oxide (OG) inks were prepared, which were deposited on vitreous carbon (CV) electrodes, followed by enzymatic immobilization. The detection capacity of the biosensors was evaluated applying electrochemical techniques. The biosensor with the best levels of detection, reproducibility and durability for the analytes under study for the detection of D-Sorbitol turned out to be that measured at a working voltage of 0.86 V vs Ag / AgCl / KCl (3 M), depositing 20 µL of OG ink and using a dilution of 0.5 µL / 100 µL of (alcohol oxidase / PBS). In the case of Maltitol the best designed biosensor was worked at 1.06 V vs Ag / AgCl / KCl (3 M), depositing 20 µL of OG ink and using a dilution of 2.0 µL / 100 µL of (alcohol oxidase / phosphate buffer).

Biosensor, Maltitol, D-sorbitol

Resumen

Se elaboraron sensores electroquímicos para la detección de edulcorantes artificiales (D-sorbitol y Maltitol) en soluciones acuosas. Estos compuestos son polialcoholes ampliamente utilizados en la industria alimenticia y bebidas, en sustitución del azúcar común., sin embargo, su consumo no se encuentra regulado, y el uso desmedido conlleva a consecuencias en el organismo como el aumento en los niveles de glucosa en sangre. Se elaboraron tintas de óxido de grafeno (OG), que fueron depositadas sobre electrodos de carbón vítreo (CV), posteriormente se llevó a cabo la inmovilización enzimática. La capacidad de detección de los biosensores fue evaluada aplicando técnicas electroquímicas. El biosensor con los mejores niveles de detección, reproducibilidad y durabilidad para los analitos en estudio para la detección de D-Sorbitol resultó ser aquel medido en un voltaje de trabajo de 0.86 V vs Ag/AgCl/KCl(3 M), depositando 20 µL de tinta de OG y utilizando una dilución de 0.5 µL/100 µL de (alcohol oxidasa/PBS). En el caso de Maltitol el mejor biosensor diseñado se trabajó a 1.06 V vs Ag/AgCl/KCl(3 M), depositando 20 µL de tinta de OG y utilizando una dilución de 2.0 µL/100 µL de (alcohol oxidasa/Buffer de fosfatos).

Biosensor, Maltitol, D-sorbitol

Citation: GALINDO-GONZÁLEZ, Rosario, ULLOA-VAZQUEZ, Talina, HERRASTI, Pilar, FUENTES-RAMÍREZ, Rosalba. Graphene oxide used for detection devices of artificial sweeteners not regulated in the food industry. ECORFAN Journal-Bolivia. 2019. 6-10: 13-18.

* Correspondence to Author (email: mr.galindo@ugto.mx)
† Researcher contributing as first author

Introduction

Artificial sweeteners are organic compounds that have been used to replace the use of sucrose or common sugar, preserving the sweet taste in foods, but with a lower caloric content, so they are in products recommended for People who try to lose weight and those with problems of hyperglycemia or diabetes. If the sweeteners are not used in the right portions can trigger effects on the organism as an alteration of blood glucose levels, risk of obesity, hypertension, metabolic disturbances and cardiovascular complications.

There are many sweeteners, among which we find alcohols sweetened or polyalcohols, this type of compounds are characterized because they are assimilated in a partial or slower than the sugar in the organism. Two polyalcohols were selected for this work: D-sorbitol (e-420) and Maltitol (e-965), both are long-chain branched alcohols and are commonly used in a wide variety of foods such as energy drinks, biscuits, cereals, Chewing, among many others.

Currently there are no rules or regulations that require producers to denote polyalcohols as such in the nutritional and energy labels of their food and beverages, instead, are categorized along with many other molecules such as Carbohydrates. The result of the lack of regulation of this type of compounds is that people do not know that they consume them, nor the proportion in which they do; So your intake can be a health risk factor. (Mexican Diabetes Federation, 2016).

Therefore, it is of great importance to take control of the consumption of these polyalcohols, which is achieved through monitoring within the production processes in the food industry.

One of the simplest technologies to carry out the monitoring of different chemicals is through the sensors, which carry out a rapid, economical and quantitative analysis of the analyte in question, which is why they become highly options Viable for the detection of chemicals and biomolecules in the environment, the food industry and clinical analyses (Sassolas, Blum, and Leca-Bouvier, 2012).

Among the different types of sensors known, the type of electrochemical detection are the most used because they have advantages such as low manufacturing and maintenance costs, require small volumes of samples, present sensitive Detection levels and enormous diversity for analyte detection (Alegret, Del Valle, & Merkoci, 2004).

Depending on the type of analyte that needs to be quantified, the most appropriate type of sensor will be selected; Many of the substances that are evaluated are usually biomolecules or other biological type, in these cases the detection response can be improved in a remarkable way including in the sensor receptor biological elements such as enzymes, antibodies, proteins, among many others; The type of sensor formed by biological elements is known as biosensor. Normally enzymes are the biological elements most used for the construction of biosensors, mainly due to their selective and catalytic properties.

Electrochemical sensors have a predominant position in the analytical instrumentation market; These are very simple technologies that do not need sophisticated measuring equipment, use very common instrumentation in laboratories such as potentiometers and Potenciostatos; The translated signal is of electrical type and easily processable by electronic methods. They are easily miniaturized devices, which allows to make measurements in small sample volumes or in areas of reduced dimensions. They present sufficient detection limits for a large majority of analytical interest samples and a wider response interval than most other types of sensors. They can be manufactured in series production techniques, with low costs and become commercialized as disposable devices without having to give them constant maintenance (Alegret, Del Valle, & Merkoci, 2004).

In a traditional way, the sensor area has used carbon-based materials such as vitreous carbon electrodes, carbon fibers and pyrolytic graphite; However, today it has been sought to introduce carbon-based nanomaterials (Yang, Denno, & Pyakurel, 2015); Such is the case of graphene oxide and graphene, which have been used mainly to carry out the immobilization of the bioreceptors.

ISSN-On line 2410-4191

So far the most studied electrochemical biosensor based on Grafíticos materials is the one that uses the enzyme glucose oxidase for glucose detection (Lawal, 2015).

However, the presence of grafíticos materials has shown increases in sensitivity, selectivity, and reproducibility of many sensors; When it has worked on the electrochemical detection of analytes such as (Bahadir & Sezgintürk, 2016), (Sassolas, Blum, and Leca-Bouvier, 2012): cholesterol, uric acid, ascorbic acid, hydrogen peroxide, methanol and glucose to name a few.

This paper presents a comparison between graphene and graphene oxide modified with the enzyme alcohol oxidase, for the elaboration of an electrochemical detection device, using synthetic samples of D-sorbitol and Maltitol, two sweeteners Widely used in the food industry, thus generating a simple, economical and effective alternative for quality control in the food industry.

Methodology

Synthesis of graphene oxide

The synthesis of graphene oxide was carried out following the technique reported by Hummer & Offeman (Ramos-Galicia, 2014), which consisted of the following steps: In a three-mouth flask placed in an ice bath, 46 ML of sulphuric acid (karal reactive) was added. To reach a temperature of 0 º C, at this time 2 g of graphite (Electron Microscopy Science #70230) were added and immediately afterwards, 6 g of potassium permanganate (Sigma-Aldrich reagents) was added. Once the previous components were mixed, the reaction was carried at a temperature of 35 º C with magnetic agitation, reached this value, it was allowed to react for 2 hours. After this time the heating was removed and the flask was slowly added to 92 mL of distilled water, leaving the solution to react for 15 minutes with magnetic agitation.

Independently in a beaker, 270 ml of distilled water and 10 ml of hydrogen peroxide were added; After 15 minutes in magnetic agitation of the product obtained from the synthesis, this solution was mixed together with the hydrogen peroxide preparation. Later, the final solution was filtered until a neutral PH was obtained.

To this point graphite oxide has been obtained, which was allowed to dry at 65 º C for 12 hours.

To obtain GO a solution of (0.1 g/10 ML) of graphite oxide and distilled H_2O was prepared respectively, the solution was soniced in an ultrasonic bath (model 1510R-MTH, at a frequency of 50-60 Hz) for a time of 4.5 hours. Finally, the solid product was separated by centrifugation, dried and ground until reaching a diameter of 75 microns (mesh #200). Two different lots were prepared to generate enough work material.

Biosensors preparation

It begins by describing the preparation of the ink of carbon-based materials, then this ink is deposited on the surface of a vitreous carbon electrode (CV), the next stage in the elaboration is the immobilization of the enzyme alcohol oxidase AlOx and Finally, the biosensor test is carried out in synthetic solutions of each one of the analytes under study. The modification of the CV electrode consisted of several deposits of 10 µL of ink in the form of layers. During each tank a vacuum oven was used at a temperature of 60 º C, which allowed each layer to be completely dried in order to carry out the next addition. It is important to leave the modified electrode for a day so that the ink anchorage to the glassy carbon electrode is as strong as posible.

Electrochemistry test

The electrochemical characterization of the modified electrodes was used a reference electrode of Ag/AgCl/KCl (3 M) and as a counterelectrode a platinum wire; The working electrode used was the developed biosensor.

Results

Figure 1 presented the Raman spectra made to the original material used that was the graphite (black line), and the samples of graphene oxide (blue line) and reduced graphene (pink line) synthesized during the investigation. In this analysis it is possible to see that the graphite has a high degree of grafítica orientation reflected in the intensity of the G-band. The defects in its structure are minimal and are manifested in the peak D1 with weak intensity.

ISSN-On line 2410-4191

The ratio of area D1/G is 0383, which is interpretable as a material of low structural disorder.

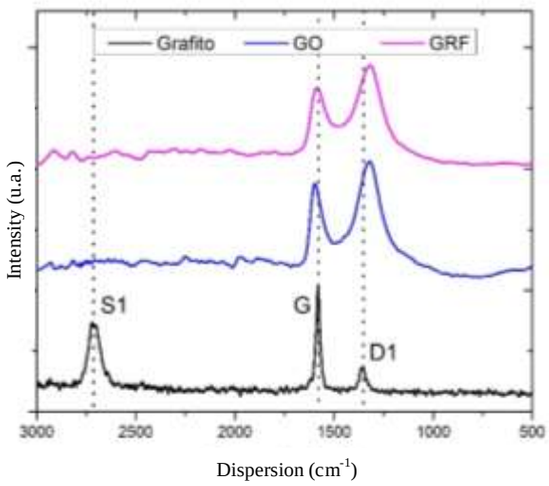

Figure 1 Raman spectra for different grafíticos materials

The G-band corresponds to the vibration within the aromatic layers in the graphite structure, its magnitude corresponds to the vibration of the C-C type SP2 hybrid link stretch. In the spectrum of the GO the G-band decreases, while the intensity of D1 increases markedly, the peaks become wider due to factors such as the presence of vacancies, defects in the structure, finite size of the net or others; They specifically represent the loss of symmetry due to the finite size of the graphite crystals or the vibration of the stretching of the hybrid links type SP2 and SP3 of the carbon atoms.

When the D1 band is intense and broad as in the case of GO, this implies that the carbonaceous material lacks ordering in its atoms (Beyssac, Goffé, & Chopin, 2002). Mainly this band is attributed to structural defects or the presence of Heteroatoms (O, H, N), resulting from the oxidation process to which the graphite was subjected. The ratio D1/G for GO is 0968 because the number of defects is higher by oxidation compared to graphite.

Figure 2 corresponds to the TEM micrographs of graphene oxide, as you can see its morphology is of type flakes with at least a length of 1 micron of approximately width.

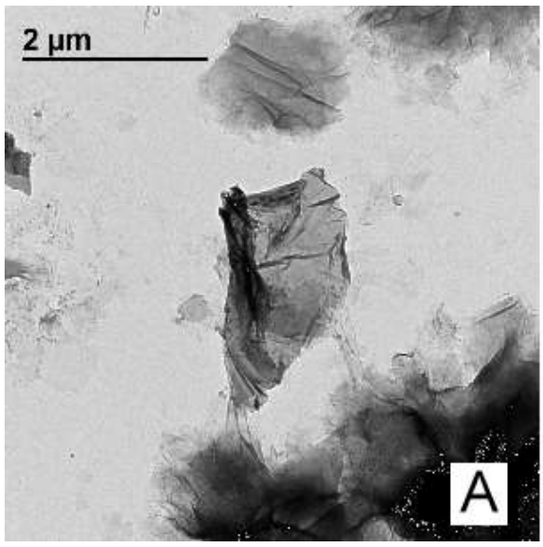

Figure 2 TEM of Grafene oxide

Figure 3 A represents an average of the cronoamperometrías obtained and B shows the calibration curve with the standard deviation of the values obtained for the biosensors.

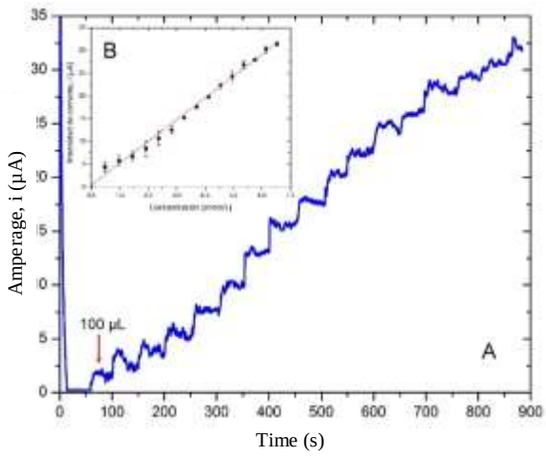

Figure 3 Results of Repetividad tests in the best conditions for sorbitol detection. A) average Cronoamperometría using a CV electrode with 20 µ L of TGO, 10 mL PBS PH = 7.4, E_w =0.864 V vs Ag/AgCl/KCl (3 M), (0.5 µ l AlOx/100 MLPBS), B) linear approximation of response detection vs. Signal Current measurement

For these biosensors the following average values were obtained: sensitivity of 4.834.83 µA/mmolL^{-1}, minimun detection limit of 0.49 mmol/L maximun 6.52 mmol/L and linear approximation factor of 0.993. The average cronoamperometría has a signal-to-noise ratio of 1.63.

The Figure 4 A represents an average of the cronoamperometrías obtained B shows the calibration curve with the standard deviation of the values obtained for the biosensors

ISSN-On line 2410-4191

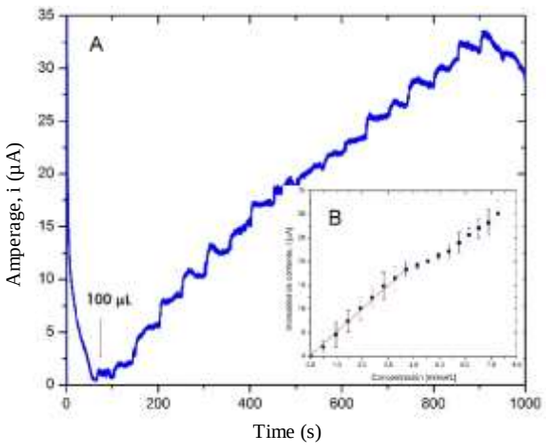

Figure 4 Results of Repetividad tests in the best conditions for maltitol detection. A) Cronoamperometry using a CV electrode 20 µL de TGO, 10 mL PBS pH=7.4, E_w=1.064 V vs Ag/AgCl/KCl(3 M), (2.0 µL AlOx/100 µL PBS), B) linear approximation of response detection vs. Signal Current measurement

For these biosensors the following average values were obtained: sensitivity of 4.92 $\mu A/mmolL^{-1}$, minimun detection limit of 0.49 mmol/L and maximun 3.70 mmol/L and linear approximation factor of 0.991. The average cronoamperometría has a signal-to-noise ratio of 1.09.

Conclusions

The GO is synthesized by means of a modified Hummer technique. In the analyses carried out to carry out the characterization, it was found that the oxidation of the material had been carried out in a satisfactory way, since they were inserted in the structure different oxygenated groups. The insertion of the oxygenated groups was also observed in the Raman spectroscopy, reflected in the variation of the width and intensity of the bands G and D1 when compared with those of graphite, which was interpreted as a loss of the crystallinity of the material. The TEM microscopies allowed to visualize that the GO presents a flake structure and with an approximate size to 1 micron. The electrochemical impedance spectroscopy made it possible to conclude that the GO is a material that contributes a resistance of 200 Ω once its ink is deposited and tested in the biosensor.

Given the characteristic parameters reported for each biosensor can be concluded, that the electrochemical detection of sorbitol is much better than that of maltitol, because the chemical structure of sorbitol is mostly akin to AlOx to be oxidized.

Therefore, the biosensor sheds more stable, reproducible responses with greater signal/noise ratios

References

Alegret, S., Del Valle, M., & Merkoci, A. (2004). Sensores electroquímicos. Barcelona, España: Materials 147.

Araújo, J. R., Martel , F., & Keating, E. (2014). Exposure to non-nutritive sweeteners during pregnancy and lactation: Impact in programming of metabolic diseases in the progeny later in life. Reproductive Toxicology, 196-201.

Azevedo, A., Prazeres, M., Cabral, J., & Fonseca, L. (2005). Ethanol biosensors based on alcohol oxidase. Biosensors and Bioelectronics, 235-247.

Badea, M., Curulli, A., & Palleschi, G. (2003). Oxidase enzyme immobilisation through electropolymerised films to assemble biosensors for batch and flow injection analysis. Biosensor Bioelectron, 689-698.

Bahadir, E., & Sezgintürk, M. (2016). Applications of graphene in electrochemical sensing and biosensing. Trends in Analytical Chemistry, 1-14.

Bartlett-Johnson, M. (07 de Marzo de 2016). Universidad Latinoamericana de Ciencia y Tecnología, Costa Rica. Obtenido de Edulcorantes Naturales y Artificiales: ¿una bendición o una maldición?: http://www.ulacit.ac.cr/files/documentosULACIT/Constant/MadisonInvestigacionEdulcorantes-QuimicaOrganica.pdf

Beyssac, O., Goffé, B., & Chopin, C. (2002). Cernat, A., Tertis, M., & Sandulescu, R. (2015). Electrochemical sensors based on carbon nanomaterials foracetaminophen detection: A review. Analytica Chimica Acta, 16-28.

Chunmei, M., Zhen, S., Changbao, C., & Zhang, L. (2014). Simultaneos separation and determination of fructose, sorbitol, glucose and sucrose in fruits by HPLC-ELSD. Food Chemistry, 784-788.

ISSN-On line 2410-4191

Cökeliler , D., & Mutlu, M. (2002). Performance of amperometric alcohol electrodes prepared by plasma polymerization technique. Anal. Chim. Acta, 217-223.

Company, T. G. (02 de Marzo de 2016). Graphene & Grafeno, The Graphene Company. Obtenido de Óxido de grafeno: http://www.oxidodegrafeno.com/es/

Wang, J., Liu, J., & Cepra, G. (1997). Thermal stabilization of enzymes immobilized within carbon paste electrodes. Anal. Chem, 3124-3127.

Wen, S., Slining, M., & Popkin, B. (2012). Use of caloric and noncaloric sweeteners in US consumer packaged foods, 2005-2009. eat rigth.

Wen, S., Slining, M., & Popkin, B. (2012). Use of Caloric and Noncaloric Sweeteners in US consumer Packaged Foods, 2005-2009. Eat right, 1828-1834.

Wikipedia La Enciclopedia libre. (30 de Marzo de 2016). Obtenido de Conductividad eléctrica: https://es.wikipedia.org/wiki/Conductividad_el%C3%A9ctrica

Yang, C., Denno, M., & Pyakurel, P. (2015). Recent trends in carbon nanomaterial-based electrochemical sensors for biomolecules: A review. Analytica Chimica Acta, 17-37.

Zhang, & Hoshino. (2014). Electrical Transducers. Electrochemical Sensors and Semiconductor Molecular Sensors. En Zhang, & Hoshino, Molecular Sensors and Nanodevices (págs. 169-225). Elsevier Inc.

Zygler, A., Wasik, A., & Namiésnik, J. (2009). Analytical methodologies for determination of artificial sweeteners in foodstuffs. Trends in Analytical Chemistry.

ISSN-On line 2410-4191

Article **ECORFAN-Journal Bolivia**
June 2019 Vol.6 No.10 19-23

Influence of NaCl on the polymerization of vinyl monomers by the suspension process

Influencia del NaCl en la polimerización de monómeros vinílicos por el proceso de suspensión

MONTERO, Erika†, CONTRERAS-LOPEZ, David, FUENTES, Rosalba and GALINDO, María Del Rosario

Universidad de Guanajuato. Departamento de Ciencias Naturales y Exactas

ID 1st Author: *Erika, Montero* / **CVU CONACYT ID:** 887231

ID 1st Coauthor: *David, Contreras-López* / **ORC ID:** 0000-0003-1384-4766

ID 2nd Coauthor: *Rosalba, Fuentes* / **ORC ID:** 0000-0003-0520-3387, **CVU CONACYT ID:** 202669

ID 3rd Coauthor: *María Del Rosario, Galindo* / **ORC ID:** 0000-0002-3612-1555, **CVU CONACYT ID:** 223987

DOI: 10.35429/EJB.2019.10.6.19.23 Received: February 09, 2019; Accepted: April 23, 2019

Abstract

The production of artificial polymers is, today, one of themost important activities of the chemical industry, polymersare widely used in everyday life, as, there are different types of polymers, they can be used for different uses. These polymeric materials have unique mechanical, physical and chemical properties, which most other materials do not possess, not to mention that its cost is lower than the other materials. The present research work focuses on the determination of optimal operating conditions for the polymerization of styrene and methyl methacrylate in a Batch reactor, as well as the influence of inorganic salt in this case NaCl in the performance of reaction and in the size of the material polymer, through the process of suspension using a synthetic route of polymerization by radical free conventional (FRP), where viscometry to the polymeric material testing was performed for this way characterize it, and to determine factors of interest such as the molecular weight, etc.

Styrene, Methyl methacrylate, Polymerization, Suspension process, Free radicals

Resumen

La producción de polímeros artificiales es, en la actualidad, una de las actividades más importantes de la industria química, los polímeros son usados ampliamente en la vida cotidiana, ya que, al existir diferentes tipos de polímeros, pueden ser aprovechados para diferentes usos. Estos materiales poliméricos tienen singulares propiedades mecánicas, físicas y químicas, que la mayor parte de otros materiales no poseen, sin mencionar que su costo es menor al de otros materiales. El presente trabajo de investigación se enfoca en la determinación de condiciones de operación óptimas para la polimerización de estireno y metacrilato de metilo en un reactor Batch, así como también la influencia de una sal inorgánica en este caso NaCl en el rendimiento de reacción y en el tamaño del material polimérico, mediante el proceso de suspensión utilizando una ruta sintética de polimerización por radicales libres convencionales (FRP), donde se le realizaron pruebas de viscosimetria al material polimérico para de esta manera caracterizarlo , y poder determinar ciertos factores de interés como el peso molecular, etc.

Estireno, Metacrilato de metilo, Polimerización, Proceso de suspensión, Radicales libres

Citation: MONTERO, Erika, CONTRERAS, David, FUENTES, Rosalba and GALINDO, María Del Rosario. Influence of NaCl on the polymerization of vinyl monomers by the suspension process. ECORFAN Journal-Bolivia. 2019. 6-10: 19-23.

* Correspondence to Author (email: david.contreras@ugto.mx)
† Researcher contributing as first author.

Introduction

Polymers, synthetic or natural are present in every aspect of our lives, in many modern materials, pharmaceutical equipment, electronic devices, automotive parts, medical equipment, etc. From time to date, polymers have been replacing traditional materials, mainly at low cost and the possibility of being adapted in a host of special applications.

Therefore, at present, the polymers area in the world is one of those with the highest growth due to the demand of its products in the international market, which is why this sector needs to invest in research and technology to improve the processes of obtaining their products.

In the present research work the synthesis of the polymers was carried out by means of the process of free radical suspension (FRP), it is a very important commercial process for the preparation of polymers with high molecular weight because it can be used for the polymerization of a wide variety of vinyl monomers under moderate reaction conditions, requiring absence of oxygen, but is water tolerant, and can be carried out over a wide range of temperatures (-80 to 250˚C).

Radical polymerization, like other chain growth polymerization mechanisms, has three main reactions: initiation, propagation and termination.

The initiation of a free radical polymerization consists of two steps. In the first, the initiator (I) is broken down into two radical species. In the second step of the initiation, a monomer molecule (M) reacts with the radical initiator to form a radical monomer. Propagation is the growth of the active chains (radicals) by a sequential addition of monomers. And the termination produces dead polymer chains: the growth of the polymer chains is finished and the active centers are irreversibly annihilated.

As mentioned in this work we focus on the suspension polymerization, where the monomer to be polymerized has to be dispersed in the continuous phase (aqueous phase) as small droplets.

To achieve a stable dispersion with a controlled coalescence of the droplets during the polymerization process, this is achieved by applying a suitable method of agitation in the reactor and by means of the use of suspending agents (stabilizing or dispersing agents).

Both the production of polystyrene (PS) and polymethyl methacrylate (PMMA) are some of the most important polymeric materials available today, so the industrial production of PS and PMMA has led to a large amount of development and sustainable growth as a mature technology.

Overall objective

Obtain polymers of styrene and methyl methacrylate by the process of suspension via free radicals, varying the reaction parameters, such as temperature, speed of agitation, etc. To determine the performance of the reaction.

Specific objectives

- Synthesize polystyrene beads, determining the optimal operating conditions for subsequent characterization.
- Synthesize polymethyl methacrylate beads to determine optimal operating conditions for further characterization
- Determination of the reaction yield.

Materials and methods

REAGENTS

Monomers> Styrene and methyl methacrylate: With a purity percentage> 99% (Sigma-Aldrich).

Washing> Hydroxide sodium 0.1M (HYCEL)

Dispersing agent> Polyvinyl alcohol (PVA). Hydrolysis percentage: 87-90%. (Sigma-Aldrich).

Initiator> Benzoyl peroxide: With a purity percentage of 97%. (Sigma-Aldrich).

Solvent> Toluene.

ISSN-On line 2410-4191

MONTERO, Erika, CONTRERAS, David, FUENTES, Rosalba and GALINDO, María Del Rosario. Influence of NaCl on the polymerization of vinyl monomers by the suspension process. ECORFAN Journal-Bolivia. 2019.

Polymerization of styrene

Determination of operating conditions: The polymerization process was followed by suspension via FRP. The reactions were carried out in a 500 mL Batch reactor, using for the continuous phase a constant volume of 240 mL of distilled water with a PVA concentration of 5 g / L, and adding different amounts of salt (NaCl), 0 g, 0.3 g, 0.45 g. While for the dispersed phase, 20 mL of styrene was added, with equal amounts of initiator (BPO); 0.325 gr (ratio 1: 130). The synthesis was carried out with a stirring speed of 150 rpm at a temperature of 85 ± 5 ° C for 2.45 hours and 3.00 hours consecutively.

Polymerization of methyl methacrylate

In the same manner, for this reaction, suspension polymerization was followed via FRP. The reactions were carried out in a 300 mL reactor, and using a constant volume of 110 mL of distilled water with a PVA concentration of 5 g / L for the continuous phase, and adding different amounts of salt (NaCl), 0 g and 0.3 g. While for the dispersed phase, 8 mL of methyl methacrylate was added, with an amount of initiator (BPO); 0.1818 gr (ratio 1: 100) and. The synthesis was carried out with stirring speeds of 420, 500 rpm at a temperature of 75 ± 5 ° C, for 1.00 hours and 1.30 hours consecutively.

Performance of the reaction

The yield of polystyrene and polymethyl methacrylate obtained with the following equation was calculated.

$$\%R = \frac{W_{MO}}{W_P} x100$$

Where:

% R is the percentage of performance

W_{MO} is the weight of the polymer obtained, gr in the reaction.

W_P is the weight of the monomers obtained theoretically in, gr.

Characterization

Viscosimetry The average molecular weights were determined with an Ostwald viscometer number 150 and the Mark-Houwink equation. The constants used for toluene styrene systems: $\alpha = 0.62$ $k = 0.037$ and for the methacrylate methyl-toluene system: $\alpha = 0.73$ $k = 0.0071$.

Results and Discussion

Experimentally, the reactions were performed with the styrene and methyl methacrylate monomers with different volumes of PVA and BPO, in a Batch reactor, at different stirring speeds of 150, 420 and 500 rpm and at 85 ± 5 °C.

The variations were made in each of the reactions until obtaining the optimum conditions of operation where pearls were obtained with good appearance and of considerable size and the reactions that were more favourable of the different polymers were selected and analysed.

The influence of temperature and polymerization time on the final molecular weight is not so significant when adding the inorganic compound (sodium chloride, NaCl) in the reaction medium, so it was not considered in the analysis of results. however, the influence that the agitation speed has if it is of consideration.

For example, the **Table 1** and **Figure 1** show the data obtained from the capillary viscosimetry to determine the molecular weight of the PS at 150 rpm and 0 g of NaCl added in the reaction medium.

Concentration (g/mL)	η_r (t/t_0)	η_{sp} ($t-t_0/t_0$)	η_{red} (η_{sp}/c)	η_{inh} In η_r/c
0.002	1.06	0.06	27.85	27.10
0.001	1.04	0.04	38.35	37.63
0.0005	1.03	0.03	50.66	50.04
0.00025	1.02	0.02	76.14	75.42

Table 1 100% Polystyrene

ISSN-On line 2410-4191

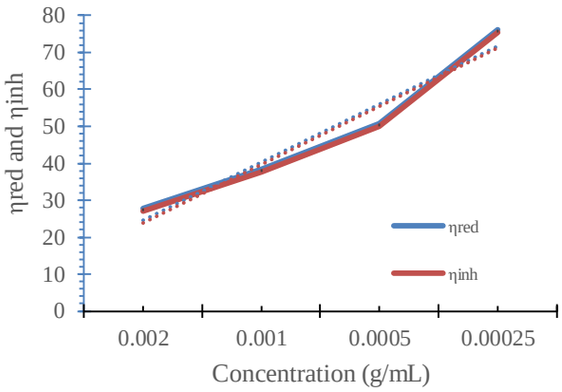

Graph 1 100% Polystyrene

The determination for molecular weight was made using the parameters offered by the Mark-Kouwink expression, that is (see **Table 2**):

[η]	α (Toluene at 298°K)	*k* PS (10^{-3})	M_v (([η]/K)^(1/α))	M_w (1.2M_V)
76.17	0.62	37	1013x10^3	1317x10^3

Table 2 100% Polystyrene

The yield of polystyrene obtained was 56.8% which is an average performance can be considered good, so we would have to check or refine some details technically. The M_w was 1317x10^3 g/mol which is a very high molecular weight.

As a summary form, **Table 3** shows the molecular weights for the polystyrene obtained by the suspension process at different reaction rates and amounts of the inorganic salt.

Rx	NaCl (g)	*Reaction rate (rpm)*	M_w x 10^{-3} (g/mol)
1	0	150	1316
2	0	420	385
3	0	500	191
4	0.3	150	539.8
5	0.3	420	245.6
6	0.3	500	125
7	0.6	150	658.5
8	0.6	420	318.7
9	0.6	500	131.7

Table 4 Summary of the molecular weights for the PS by the process of suspension at 85 °C

The influence of the rate of agitation and the amount of sodium chloride in the reaction medium can be seen in **Figure 2**, clearly observing how the flocculating effect of the inorganic salt (cage effect) remains very intense as the amount of ions in the reaction medium; however, there is a limit of this amount and it is observed with 0.6 g of NaCl.

This is because the medium is already saturated, the effect is already minimal with the size of the polymer chain, which no longer allows it to continue to grow in the process of chain propagation.

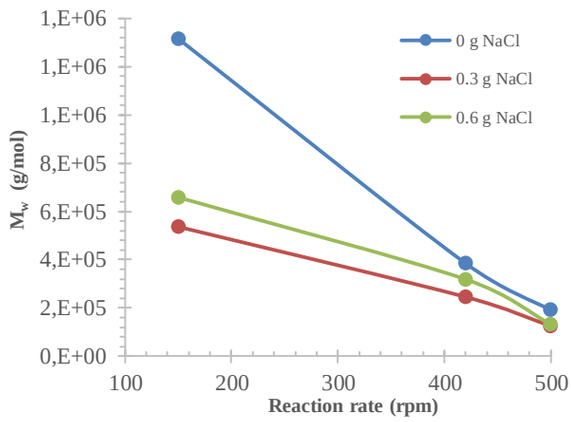

Graph 2 Evolution of the Mw of the PS in the process of suspension at different concentrations of NaCl and agitation speed at 85 ° C

The tendency that can also be observed is that as the speed of agitation increases in the medium, the molecular weight decreases, which is correct because there is a greater breakage of the pearls formed in the process of suspension; that is, the size of the particles is smaller as the agitation speed increases, so there is less volume to store a greater amount of monomer. Likewise, coupled with the presence of NaCl, the space is diminished and therefore, there is a lower molecular weight of the polymer chains formed.

Similarly, **Table 5** presents the data acquired for PMMA at 85 ° C of molecular weight at different inorganic salt concentrations and agitation rates.

ISSN-On line 2410-4191

Rx	NaCl (g)	*Reaction rate (rpm)*	M_w x 10^{-3} (g/mol)
10	0	150	1586.1
11	0	420	457.7
12	0	500	206.6
13	0.3	150	781
14	0.3	420	392.1
15	0.3	500	183
16	0.6	150	693.1
17	0.6	420	359.8
18	0.6	500	149.7

Table 5 Summary of the molecular weights for the PMMA by the process of suspension at 85 ℃

The yield of methyl polymethacrylate obtained was 77% average which is a yield under the operating conditions were favorable for the reaction. Considering that the propagation constant that MMA has is much greater than that of styrene, which denotes that the reaction time is shorter to obtain this conversion; Likewise, a similar behavior is observed in the evolution of molecular weight with respect to the agitation value and the concentration of the inorganic salt (see **Figure 3**).

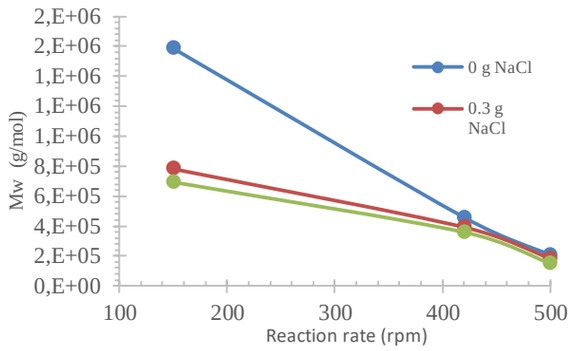

Graph 3 Evolution of the Mw of the PMMA in the process of suspension at different concentrations of NaCl and agitation speed at 85 ° C

However, the effect of sodium chloride as a flocculating effect in MMA is not very appreciable at high concentrations and this is due to the electrostatic forces presented by the inorganic salt with the ester group present in the monomer, indicating that the critical concentration in this case is 0.3 g NaCl.

Conclusions

By way of conclusion we can say that through this work it was observed that for the polymerization performance of styrene and methyl methacrylate it is important, the presence of the dispersing agent since it avoids the agglomeration or coalescence of the polymer beads.

Because when decreasing this agglomeration we will have mostly pearls and a better performance in the reaction, with respect to the inorganic salt that in our case the NaCl, we can say that it was mostly favorable in the styrene polymers, not so much for the methyl methacrylate, but in if it is a good influence on the size of polymeric material and influences its consistency.

Another important factor is the agitation speed that influences the formation of beads and molecular weight. Based on this, it was possible to obtain the most adequate operating conditions for the process, giving as a good result that the suspension process is a good way to obtain this type of polymers.

Acknowledgements

David Contreras-López acknowledges the financial support of this research by CIIC-2019 UGTO through the grant for project "*Interacción de nanopartículas de óxidos metálicos soportados en matrices poliméricas para el desarrollo de compositos conductores*"

Also, to the M.C. **Claudia Cecilia Rivera-Vallejo** of the CIQA for the determination of the molecular weights of the polymeric samples.

References

Matyjaszewski, K. et al. Handbook of radical polymerization Wiley-Interscience, 2002.

https://books.google.com.mx/books?isbn=8428333084-José Antonio Fidalgo Sánchez, Manuel Fernández Pérez, Fernández Noemí Fernández - 2016

Tesis- Polímeros: Albert van den Berg and T.S.J. Lammerink, Micro Total Analysis Systems: Microfluidic Aspects, Integration Concept and Applications

Frías, C., Ize-Lema, I., y Gavilán, A. (2003). La situación de los envases de plástico en México. Gazeta Ecológica, 69:67-82.

[5] 3. - R. Sandler, Stanley. 1998. Polymer synthesis and Characterization. 14-16.

Article **ECORFAN-Journal Bolivia**

June 2019 Vol.6 No.10 24-31

Nanocristal and ferrite numerical comparison for high frequency and low power electronic converters

Comparación númerica de núcleos de nanocristal y ferrita para convertidores electrónicos de alta frecuencia y baja potencia

CASTILLO, Ibsan, PEREZ, Francisco, RODRIGUEZ, Martin, CAMINO, Pedro and FRANCO, Carlos

Celaya Insitute of Technology - Grupo SSC

ID 1st Author: *Ibsan, Castillo* / **ORC ID:** 0000-0002-4740-485X, **CVU CONACYT ID:** 785019

ID 1st Coauthor: *Francisco, Perez* / **ORC ID:** 0000-0002-6116-6464, **CVU CONACYT ID:** 203899

ID 2nd Coauthor: *Martin, Rodriguez* / **ORC ID:** 0000-0003-2178-4804, **CVU CONACYT ID:** 357742

ID 3rd Coauthor: *Pedro, Camino* / **ORC ID:** 0000-0002-1576-9846, **CVU CONACYT ID:** 667169

ID 4th Coauthor: *Carlos, Franco* / **ORC ID:** 0000-0002-2492-4756, **CVU CONACYT ID:** 94853

DOI: 10.35429/EJB.2019.10.6.24.31 Received: March 09, 2019; Accepted: May 30, 2019

Abstract

This paper presents the numerical comparison in ANSYS Maxwell between nanocrystalline, Vitroperm 500F, and ferrite, 3C90, cores to be used in power electronic converters (PECs) transformers. The converter topology used is the doubled switch Forward, due to its characteristics and its power range (<500W). The transformer model development, the characterization and the BH measure curves from the material, as well as its validation and the excitation type implemented in the numerical model are described in the methodology. The exposed results show an improvement in comparasion with the ferrite, in addition to a better flexibility in the magnetic design methodology, given by the nanocrystalline magnetic characteristics.

Nanocrystalline, ANSYS, Forward

Resumen

El articulo presenta la comparación numérica en ANSYS Maxwell entre núcleos de nanocristal, Vitroperm 500F, y ferrita, 3C90, para ser usados en transformadores para convertidores electrónicos de potencia (CEP). La topología de convertidores usada es el Forward con doble interruptor, debido a sus características y su rango de potencia (<500W). El desarrollo del modelo del transformador, la caracterización y medición de curvas BH del material, asi como su validación y el tipo de excitación implementados en el modelo númerico son descritos en la metodología. Los resultados expuestos muestran una mejora en el uso de nancristales en comparación con la ferrita, así como mayor flexibilidad en la metodología de diseño magnético dadas las características del material nanocristalino.

Nanocristal, ANSYS, Forward

Citation: CASTILLO, Ibsan, PEREZ, Francisco, RODRIGUEZ, Martin, CAMINO, Pedro and FRANCO, Carlos. Nanocristal and ferrite numerical comparison for high frequency and low power electronic converters. ECORFAN Journal-Bolivia. 2019. 6-10: 24-31.

* Correspondence to Author (email: M1703083@itcelaya.edu.mx)
† Researcher contributing as first author.

Introduction

Today, electronic power converters (PECs) have increased the operating frequency and reduced the size of the entire system [1]. This can be achieved due to the advancement in the technology of power electronic switches, such as silicon carbide (SiC). The increase in switch technology reduces switching losses [1], which is one of the major considerations by increasing the operating frequency; by increasing the working frequency, the magnetic components can be reduced in size, but the losses in the nucleus increase.

Current materials used in magnetic devices, such as ferrite, have a rather low saturation point which represents an impediment to reduce the size of magnetic devices. That is why the tendency in PECs is to find and use new magnetic materials that can work in smaller sizes and with better performance [2]. New magnetic materials with higher saturation points, wider frequency operating ranges, smaller core losses and small magnetostriction are required. The characteristics of magnetic materials with nanocrystals make this type of candidate materials to migrate from conventional materials, this has led to their potential applications being studied.

In [3] a magnetic nanocrystal stator is constructed and analyzed to reduce the losses in the stator of an electric machine. The shape of the stator core is not commercial and this configuration and special cutting was done by the Hitachi company. The results in [3] show a reduction in core losses from 64% to 75% compared to conventional silicon steel material.

Another application is shown in [4]. In this research, the authors analyzed and designed a high density transformer for a resonant converter (30 kW 200 kHz). At work it can be clearly seen a decrease in size by comparing the nanocrystalline and ferrite material, almost 50% in size. The tests performed on the transformer confirmed an improvement in the performance of the transformer by using magnetic materials with nanocrystalline structures, reducing losses, increasing power density and greater saturation of magnetic flux. While there is some research with nanocrystal magnetic cores such as those discussed in [5,6,7,8], most of the research focuses on high power.

Due to the high power, the size of the core is usually large and the cost of the nanocrystalline material is excessively high, compared to the price of ferrites. There are much smaller nanocrystalline cores that can be used in conventional low power applications with a price that can compete with that of ferrites.

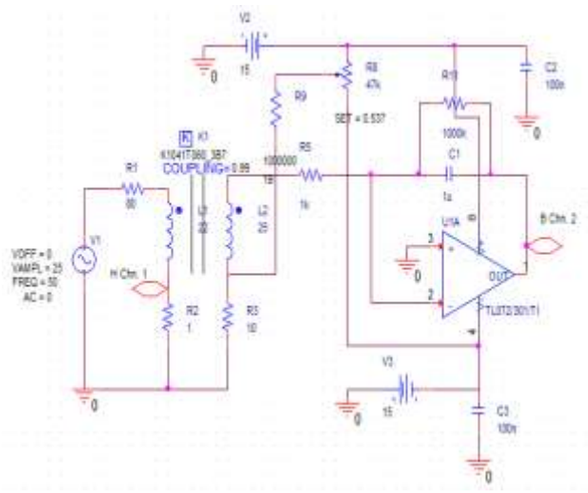

Figure 1 BH curve measuring circuit for magnetic materials

Magnetic Properties of the Cores

This section presents the circuit used to obtain the BH curves of the magnetic materials which are used in the finite element analysis in the ANSYS Maxwell software.

Figure 1 shows the circuit used for the measurement of magnetic parameters, magnetic flux density (B) and magnetic field (H). The magnetic field strength is directly proportional to the field generating current (1) and this passes through the primary of the transformer; therefore, a shunt resistor is necessary to measure the magnetic flux intensity in the core. The magnetic flux is given by the integral of the voltage induced in the secondary, which is why the operational amplifier is configured to function as an integrator and thus the magnetic flux is directly proportional to the output voltage of the operational amplifier (2).

$$H=\frac{Np*I}{Lc} \quad (1)$$

Where H is the magnetic field strength, Np is the number of turns in the primary and Lc is the length of the magnetic path of the core.

$$B=\frac{\Phi}{Ac} = -\frac{Vo*C1*R6}{Ns} \quad (2)$$

CASTILLO, Ibsan, PEREZ, Francisco, RODRIGUEZ, Martin, CAMINO, Pedro and FRANCO, Carlos. Nanocristal and ferrite numerical comparison for high frequency and low power electronic converters. ECORFAN Journal-Bolivia. 2019.

Where B is the magnetic field density, Ac is the cross-sectional area of the core, Φ is the magnetic flux, Vo is the output voltage of the operational amplifier, C1 and R6 are the elements of the integrated and Ns is the number of turns in the secondary.

An oscilloscope is necessary where the channels can be used as axes, since channel one will be connected to the shunt resistor and channel two to the output of the operational amplifier. Figures 2 and 3 show the BH curves of the Vitroperm 500F material and 3C90 ferrite respectively, which were measured at 500 Hz and at 28.5 ° C.

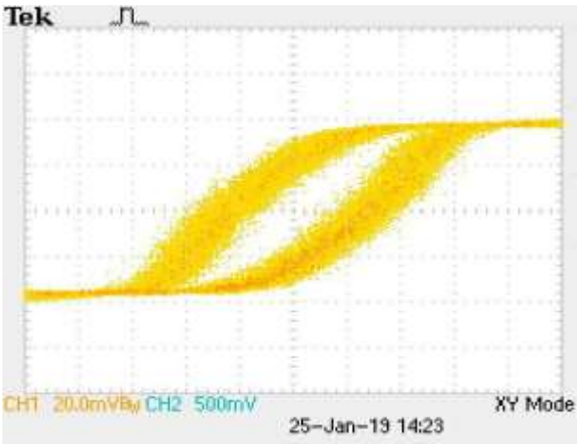

Figure 2 BH curve of the Vitroperm 500F material at 500Hz and 28.5 ° C

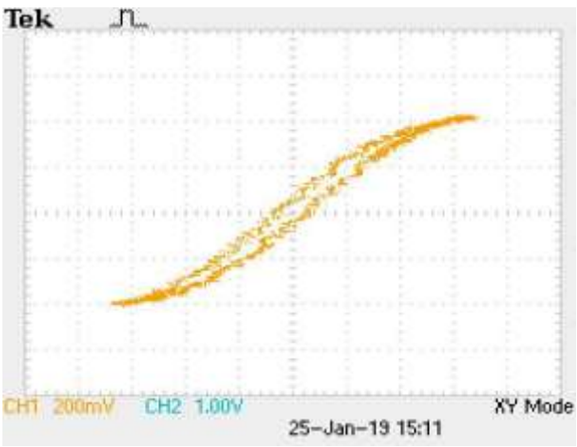

Figure 3 BH curve of the 3C90 ferrite at 500Hz and 28.5 ° C

Finite Element Analysis (FEA)

In this section all the details for the numerical simulation are described. The main design parameters are shown and how the model will be analyzed is created. It is important to present the considerations to simulate a numerical model in the most optimal way.

Therefore, a 2D model is presented in this section. The materials used in the 2D model, as well as the validation to use it are described. It is necessary to validate all material used in an analysis with reference values, usually they can be found in the manufacturer's data sheets. In the corresponding section, the values taken to validate the nanocrystal material are mentioned. Finally, the transitory design of the Forward converter is exposed; this model is created to analyze the transformer. This analysis serves to know the distribution of the magnetic flux and saturation of the nucleus. Core losses are obtained from this analysis because the power of the transformer into a Forward converter is not sinusoidal.

The design of the converter is beyond the scope of this paper, however, the methodology and analysis of the Forward topology with double switch (Figure 4) can be found in [10].

Parameter Name	Design parameters *Value*	*Unit*
Input voltage	200	V
Output voltage	50	V
Output current	10	A
Work cycle	0.25	-
Operating frequency	100	kHz
Inductor value	192	uH
Capacitor value	22	uF

Table 1 Design parameters for the Forward converter

Parameter Name	Design parameters *Nanocrystalline core*		Design parameters *Ferrite core (ETD34)*	
	Value	Unit	Value	Unit
Operating frequency	100	kHz	100	kHz
Security Saturation Point	0.8	T	0.33	T
Number of turns ratio	1	-	1	-
Area product (calculated)	0.3411	4	1.11	cm4
Area product (core)	0.4755	cm4	11.931	cm4
Number of turns in the primary and secondary coil	23	-	23	-

Table 2 Design parameters for the transformer

CASTILLO, Ibsan, PEREZ, Francisco, RODRIGUEZ, Martin, CAMINO, Pedro and FRANCO, Carlos. Nanocristal and ferrite numerical comparison for high frequency and low power electronic converters. ECORFAN Journal-Bolivia. 2019.

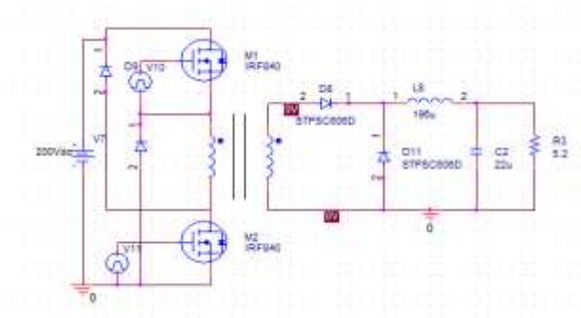

Figure 4 Forward converter with double switch

The parameters for the Forward converter are shown in Table 1. The design parameters of the nanocrystalline and ferrite transformers can be observed in Table 2. The methodology for transformer design can be found in [11] and it shows that the more magnetic flux density can be induced in a material, the smaller the cross-sectional area is needed and the smaller the size of the magnetic device.

The methodology to design an electronic power transformer and analyze it in ANSYS consists of:

1. Design the 3D or 2D model in a computer-aided design software.

2. The next step is to characterize all the materials to be used in the model.

3. Perform a frequency analysis and calculate the losses in the core to compare them with those of the manufacturer.

4. Finally, the transitional analysis model is created. With external power due to the non-sinusoidal power signals that can be observed in the converters.

2D Core and Winding Design

The geometry for nano-crystal numbers, competitive in price to ferrite, which satisfies the design requirements, is a toroidal shape. For a 500W Forward converter, the specific core of the manufacturer Vacuumschmelze is the model T6006-L2025- W523. For the ferrite, the smallest core that satisfies the requirements is the ETD34. These design features to select the cores are those shown in Table 2.

The nominal values of each core, used for the creation of the 2D and 3D model are shown in [12] and [13], for the nanocrystal core and the ferrite, respectively. Because the coating material of the nanocrystal core is considered to be permeable equivalent to that of vacuum, the plastic is created as a non-model element in ANSYS Maxwell to improve the computing speed.

The toroidal model is performed in 2D simulation because simulating the complete 3D model as shown in Figure 5 requires a large amount of computational memory, due to the small cable length. To simulate this model, the first iteration consists of approximately 1,700,000 elements. So the 2D model is recommended when the geometries prevent simplifying winding due to changes in the cross-section of the cable. In the 2D model (Figure 6) we consider that each conductor that is observed is litz cable and there is no induced skin effect on them.

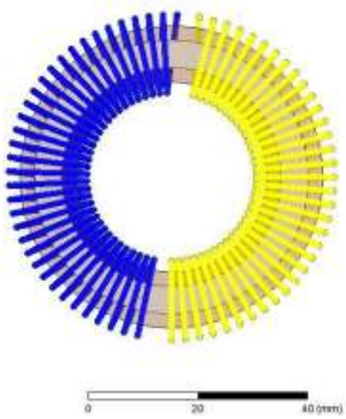

Figure 5 3D model of the toroidal transformer

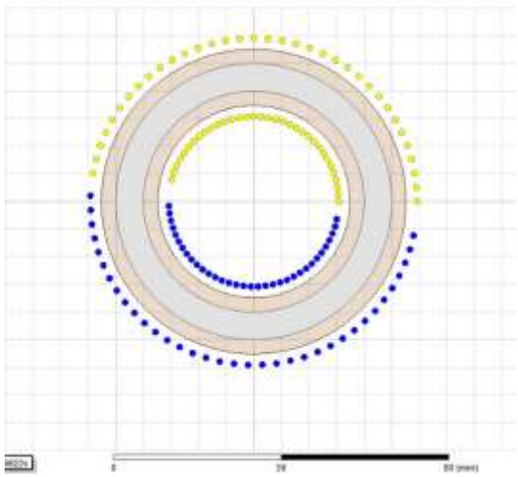

Figure 6 2D model of the toroidal transformer

CASTILLO, Ibsan, PEREZ, Francisco, RODRIGUEZ, Martin, CAMINO, Pedro and FRANCO, Carlos. Nanocristal and ferrite numerical comparison for high frequency and low power electronic converters. ECORFAN Journal-Bolivia. 2019.

In the case of the ferrite core, the winding maintains an equal cross-sectional area in all parts because it is designed as a cylinder. Therefore, this model can be simplified as a solid conductor, where the width of the conductor is given by (3).

$$h = \sqrt{(\pi / 4)} * D \quad (3)$$

Moreover, due to the symmetry stored by the ETD34 core, it is possible to cut the model and simulate only 1/4 of the complete geometry without compromising the system response. The final simulation model for the ferrite core can be seen in Figure 7.

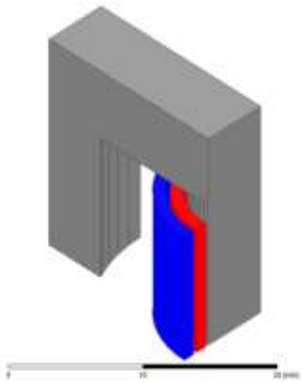

Figure 7 3D model of the transformer, ETD34 core

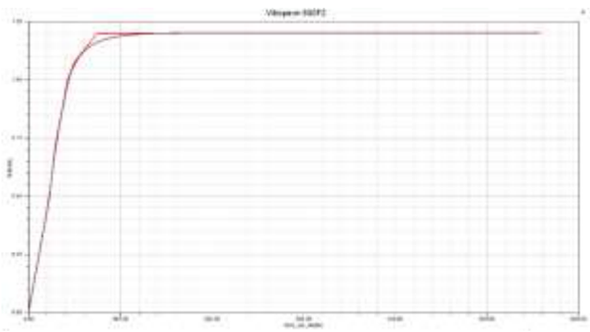

Graph 1 BH curve of the DC of the Vitroperm 500F material

Nanocrystalline Material Characterization

The characterization of ANSYS Maxwell requires giving the BH curve in DC. The BH curve of DC does not contain hysteresis to obtain said curve of the values of Figure 2; the values can be interpolated and checked with the curve given in [9]. The BH curve for the characterization of the material can be seen in Graph 1.

Given the extensive study in the field of ferrites, the ANSYS Maxwell software has in its libraries the magnetic properties of the Ferroxcube 3C90 ferrite, as well as the coefficients of the mathematical loss model, Steinmetz; therefore, it is not necessary to inquire about obtaining the parameters. However, the BH curve obtained in the measurements can be interpolated in the same way as the nanocrystal curve to check the model of the library with the physicist.

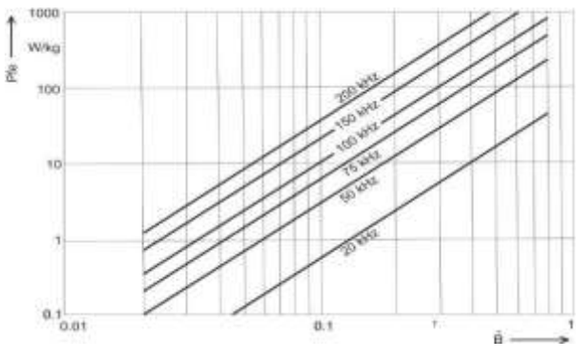

Graph 2 Loss curves vs. frequency of the Vitroperm 500F material

The loss model of Steinmetz (4) [14] is the one used in ANSYS to calculate the losses of the magnetic components. The coefficients of the Steinmetz mathematical model are obtained with the loss curves at various frequencies shown in Graph 2 and given in [15].

$$P_c = K_h * f * B_p^{\,n} + K_e * (f * B_p)^2 + K_\alpha * (f * B_p)^{1.5} \quad (4)$$

Where Kh, n, Ke and Ka are the loss coefficients, f is the operating frequency and Bp is the average magnetic flux density flowing through the core cross section.

The mathematical model of losses already considers hysteresis losses with the corresponding coefficient Kh. Density and stacking factor for laminated materials are other characteristics that are required by the software. The stacking factor can be obtained with (5). The density for the nanocrystal is 7100 kg/m^3 and the stacking factor is 0.4 and must be oriented in cylindrical coordinates on the radial axis, by toroidal geometry.

$$S_F = A_N / A_{Fe} \quad (5)$$

CASTILLO, Ibsan, PEREZ, Francisco, RODRIGUEZ, Martin, CAMINO, Pedro and FRANCO, Carlos. Nanocristal and ferrite numerical comparison for high frequency and low power electronic converters. ECORFAN Journal-Bolivia. 2019.

Where A_{Fe} is the effective cross-sectional area of the nanocrystalline material and A_N is the nominal cross-sectional area of the core.

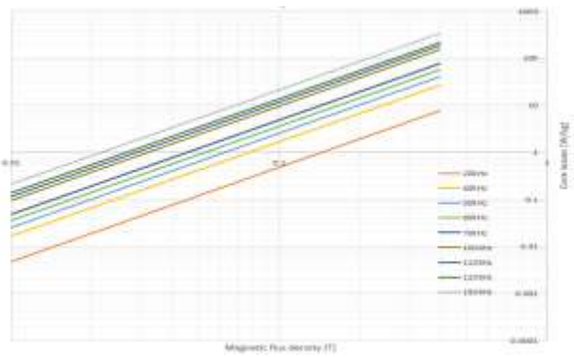

Graph 3 Loss vs. frequency curves of the Vitroperm 500F material obtained in ASYS Maxwell

Nanocrystalline material validation

To validate the material model, it is necessary to perform a frequency analysis with ANSYS Maxwell. The geometry for this simulation is the same one designed in the previous section and only one coil is used to simplify the simulation model. With this analysis, a variation is made in the input power, which is a sine wave, to vary the magnetic flux density induced in the core. To obtain the losses in the core in ANSYS Maxwell (Graph 3) it is necessary to create a line in the core cross section. To obtain a value of the magnetic flux density is used (6).

$$B=\int|\vec{B}|.ds/s \quad (6)$$

Where $\vec{B}$ is the magnetic flux density vector and s is the area of the core cross section.

Losses can be plotted for losses in the core against frequency. Comparing the graph obtained in ANSYS and the one given by the manufacturer, it can be seen how each of the curves of both graphs corresponds, so that the material has been validated with real values and can be used in the following analyzes.

Transitional Analysis Design

The Forward topology comprises a transformer used to isolate the input and output stages of one another and to increase or decrease the output voltage. The transient analysis shows the losses in the nuclei of both transformers: nanocrystal and ferrite.

In this design the excitation of the transformers is the topology of the Forward converter (Figure 4), the parameters are extracted in the circuit editor of ANSYS Maxwell. These parameters determine the amplitude and waveform of the current in the primary. Thus, the transformer can be analyzed for the application that was designed and the other elements of the converter are simulated as ideals.

Numerical Results and Performance Comparison

This section shows the results of the transitional analysis. The analysis is considered from the start of the circuit and is simulated until it reaches the steady state in order to compare the cores correctly. The time range for the simulation is from 0us to 900us, with a time step of 0.1us to ensure quality results; 9000 iterations are performed per transformer. Due to the analysis requirements, parallel processing is used in ANSYS using 9 of 10 available processor cores.

ANSYS Maxwell uses an automatic mesh refinement method, only in non-transient analyzes. Therefore, to have a quality mesh in the transitory analysis, the frequency analysis mesh has been imported, which improves the simulation time.

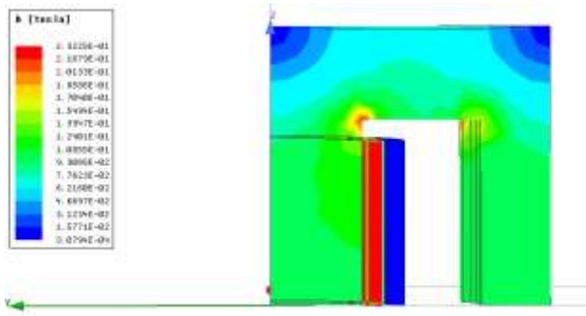

Figure 8 Density of magnetic flux in ferrite core

For both materials there are values calculated automatically by the software. The first parameter analyzed is the magnetic flux density (B), Figures 8 and 9 represent the time interval where the greatest B occurs.

CASTILLO, Ibsan, PEREZ, Francisco, RODRIGUEZ, Martin, CAMINO, Pedro and FRANCO, Carlos. Nanocristal and ferrite numerical comparison for high frequency and low power electronic converters. ECORFAN Journal-Bolivia. 2019.

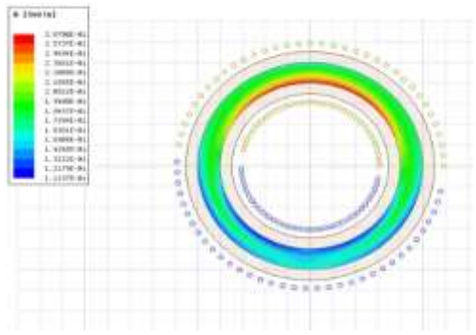

Figure 9 Magnetic flux density in nanocrystal core

A more prone to saturation nucleus in the ETD34 nucleus can be seen in Figure 8. The saturation point for the 3C90 ferrite is 0.44 T; despite this, in the design it is always advisable to consider a saturation point lower than the real one, to avoid saturating the core, in this case the saturation point fixed is 0.33 T. In Figure 8 the maximum value of magnetic flux is 0.218 T compared to the nanocrystal core B, which is 0.261 T. The saturation point for the design in the nanocrystal core was 0.8 T. By analyzing both nuclei, we can see that the most prone to saturation is the ferrite core. Figure 4 shows the output voltage of the Forward convector with a nanocrystal core. Comparing the output voltage of the nanocrystal core converter with the output voltage of the ferrite core converter (Figure 5), we can see that the latter is larger than the nanocrystal core.

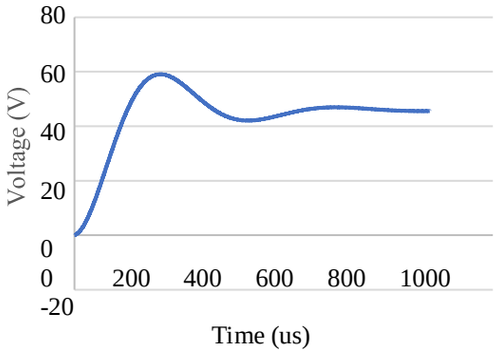

Graph 4 Output voltage of the converter with nanocrystal core

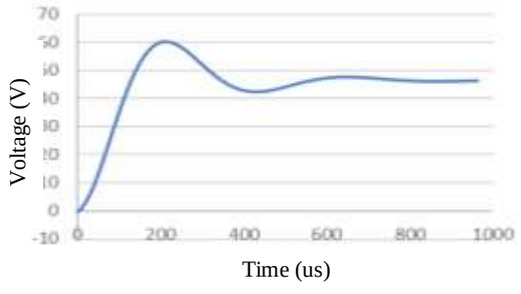

Graph 5 Output voltage of the converter with ferrite core

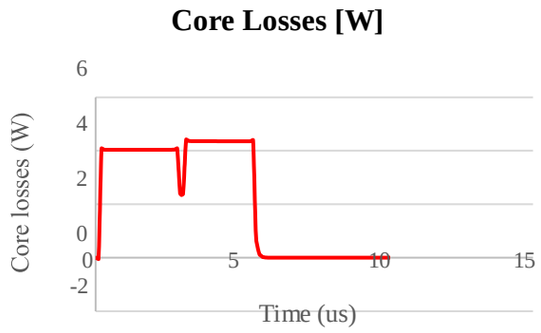

Graph 6 Loss in the nanocrystalline nucleus

Figures 6 and 7 show the losses in the transformer core built with nanocrystal and with ferrite, respectively. It can be seen that the losses in the ferrite transformer are lower than in the nanocrystal transformer. This is due to the fact that the cross-sectional area of the nanocrystal transformer is smaller, causing a higher magnetic flux density in the nanocrystal core.

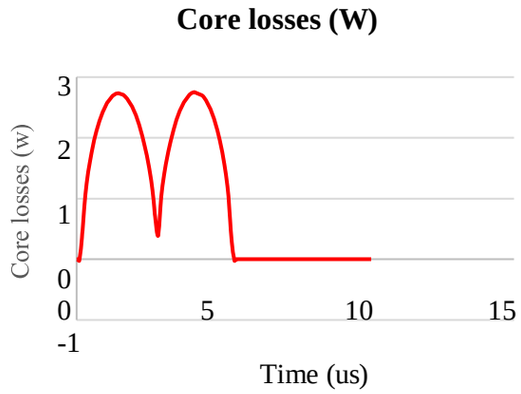

Graph 7 Loss in the 3C90 ferrite core

Given the conductivity or material, there are greater losses due to Eddy currents compared to losses of the ferrite core. The losses of the ferrite core are almost entirely attributed to the hysteresis losses of the material and turn out to be smaller than the nanocrystal core.

Conclusions

By analyzing the results obtained in the simulation, a greater flexibility in the design for the nanocrystal nuclei can be observed. Although the losses in the nanocrystalline core are greater compared to that of ferrite, the cross section of the ETD34 core is 4.9 times larger than the core cross section T60006-L2025-W523.

ISSN-On line 2410-4191

CASTILLO, Ibsan, PEREZ, Francisco, RODRIGUEZ, Martin, CAMINO, Pedro and FRANCO, Carlos. Nanocristal and ferrite numerical comparison for high frequency and low power electronic converters. ECORFAN Journal-Bolivia. 2019.

This represents a larger core and weight; the ferrite core is 3 times heavier than the nanocrystal core, and there is no smaller ferrite core that meets the design specifications of a 500W Forward converter, unless the security saturation point becomes wider, which can create the risk of saturating the core. If the cross section of the nanocrystal core doubled the losses between the cores it would be similar. The nanocrystalline core has greater flexibility in design, due to its high saturation point.

The cross section of the nanocrystalline core can be increased by saving the same dimensions specified in the data sheet, if a greater stacking factor is specified to the manufacturer to cover the cross section with more magnetic material. This type of low-cost cores are used in common mode shock, however, this article demonstrates its wide potential and improvement in power density and losses in electronic power converters, increasing the cross-section of the core to induce less losses by Eddy currents in the material.

References

[1] D. Dalal and C. Quinn, “Empowering the electronics industry: A power technology roadmap,” in Proc. IEEE Appl. Power Electron. Conf. and Exposition, Tampa, FL, 2017.

[2] W.G. Hurley. (2016, May 27). Challenges and trends in magnetics [Online]. Available: http://eznetonline.com

[3] N. Denis, M. Inoue, K. Fujisaki, H. Itabashi and T. Yano, “Iron loss reduction of permanent magnet synchronous motor by use of stator core made of nanocrystalline magnetic material,” unpublished, IEEE.

[4] W. Shen, F. Wang, D. Boroyevich and C. W. Tipton IV, "High-density nanocrystalline core transformer for high-power high-frequency resonant converter," IEEE Trans. Ind. Applicat., vol. 44, pp. 213-222, Jan. 2008.

[5] Y. Wang, G. Calderon-Lopez and A. J. Forsyth, "High-frequency gap losses in nanocrystalline cores," IEEE Trans. Power Electron., vol. 32, pp. 4683-4690, Jun. 2017

[6] R. C. Edwards and M. G. Giesselmann, "Characterization of a high power nanocrystalline transformer," IEEE 34th Int. Conference on Plasma Sci., Albuquerque, NM, 2007, pp. 869-869.

[7] K. Warnakulasuriya, F. Nabhani and V. Askari, "Development of a 100kW, 20 kHz nanocrystalline core transformer for DC/DC converter applications," PCIM Europe 2016; Int. Exhibition and Conf. for Power Electron., Intelligent Motion, Renewable Energy and Energy Manage., Nuremberg, Germany, 2016, pp. 1-8.

[8] İ. Sefa, S. Balci and M. B. Bayram, "A comparative study of nanocrystalline and SiFe core materials for medium-frequency transformers," 2014 Proc. 6th Int. Conf. on Electron., Comput. and Artificial Intell., Bucharest, 2014, pp. 43-48.

[9] EMC Products base on nanocrystalline Vitroperm®, Catalog., Vacuumschmelze, Jan. 2016. Available: www.vacuumschmelze.com.

[10] D. Hart, “DC Power Supplies,” in Power Electronics, 1st. ed. New York, Mc.Graw-Hill, 2011, ch. 7, pp. 235-330.

[11] W. T. McLyman, Transformer and Inductor Design Handbook, 3rd ed., New York: Marcel Dekker, 2004.

[12] T60006 L2025-W523, Datasheet, Vacuumschmelze, Jul. 2007. [Online]. Available: www.vaccumschmelze.com.

[13] H. Schwenk, J. Beichler, W. Loges and C. Scharwitz, "Actual and future developments of nanocrystalline magnetic materials for common mode chokes and transformers," Proc. of PCIM Europe 2015; Int. Exhibition and Conf. for Power Electron., Intelligent Motion, Renewable Energy and Energy Management, Nuremberg, Germany, 2015, pp. 1-8.

[14] X. Liu, Y. Wang, J. Zhu, Y. Guo, G. Lei and C. Liu, "Calculation of core loss and copper loss in amorphous/nanocrystalline core-based high-frequency transformer," AIP Advances, 2016.

[15] Vitroperm 500 F und Vitrovac 6030 F, Datasheet, Vacuumschmelze, 2003. [Online]. Available: www.vaccumschmelze.com.

ISSN-On line 2410-4191

CASTILLO, Ibsan, PEREZ, Francisco, RODRIGUEZ, Martin, CAMINO, Pedro and FRANCO, Carlos. Nanocristal and ferrite numerical comparison for high frequency and low power electronic converters. ECORFAN Journal-Bolivia. 2019.

[Title in Times New Roman and Bold No. 14 in English and Spanish]

Surname (IN UPPERCASE), Name 1st Author†*, Surname (IN UPPERCASE), Name 1st Coauthor, Surname (IN UPPERCASE), Name 2nd Coauthor and Surname (IN UPPERCASE), Name 3rd Coauthor

Institutional Affiliation of Author including Dependency (No.10 Times New Roman and Italic)

International Identification of Science - Technology and Innovation

ID 1st author: (ORC ID - Researcher ID Thomson, arXiv Author ID - PubMed Author ID - Open ID) and CVU 1st author: (Scholar-PNPC or SNI-CONACYT) (No.10 Times New Roman)

ID 1st coauthor: (ORC ID - Researcher ID Thomson, arXiv Author ID - PubMed Author ID - Open ID) and CVU 1st coauthor: (Scholar or SNI) (No.10 Times New Roman)

ID 2nd coauthor: (ORC ID - Researcher ID Thomson, arXiv Author ID - PubMed Author ID - Open ID) and CVU 2nd coauthor: (Scholar or SNI) (No.10 Times New Roman)

ID 3rd coauthor: (ORC ID - Researcher ID Thomson, arXiv Author ID - PubMed Author ID - Open ID) and CVU 3rd coauthor: (Scholar or SNI) (No.10 Times New Roman)

(Report Submission Date: Month, Day, and Year); Accepted (Insert date of Acceptance: Use Only ECORFAN)

Abstract (In English, 150-200 words)

Objectives
Methodology
Contribution

Abstract (In Spanish, 150-200 words)

Objectives
Methodology
Contribution

Keywords (In English)

Indicate 3 keywords in Times New Roman and Bold No. 10

Keywords (In Spanish)

Indicate 3 keywords in Times New Roman and Bold No. 10

Citation: Surname (IN UPPERCASE), Name 1st Author†*, Surname (IN UPPERCASE), Name 1st Coauthor, Surname (IN UPPERCASE), Name 2nd Coauthor and Surname (IN UPPERCASE), Name 3rd Coauthor. Paper Title. ECORFAN Journal. Year 1-1: 1-11 [Times New Roman No.10]

---

* Correspondence to Author (example@example.org)
† Researcher contributing as first author.

Introduction

Text in Times New Roman No.12, single space.

General explanation of the subject and explain why it is important.

What is your added value with respect to other techniques?

Clearly focus each of its features

Clearly explain the problem to be solved and the central hypothesis.

Explanation of sections Article.

Development of headings and subheadings of the article with subsequent numbers

[Title No.12 in Times New Roman, single spaced and bold]

Products in development No.12 Times New Roman, single spaced.

Including graphs, figures and tables-Editable

In the article content any graphic, table and figure should be editable formats that can change size, type and number of letter, for the purposes of edition, these must be high quality, not pixelated and should be noticeable even reducing image scale.

[Indicating the title at the bottom with No.10 and Times New Roman Bold]

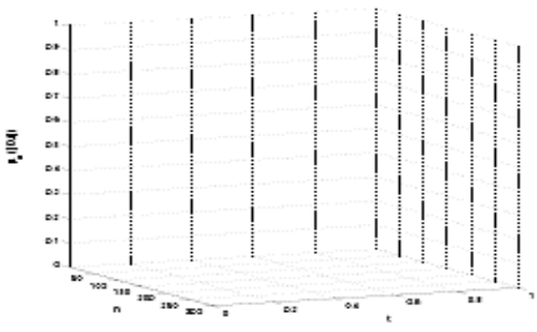

Graphic 1 Title and *Source (in italics)*
Should not be images-everything must be editable.

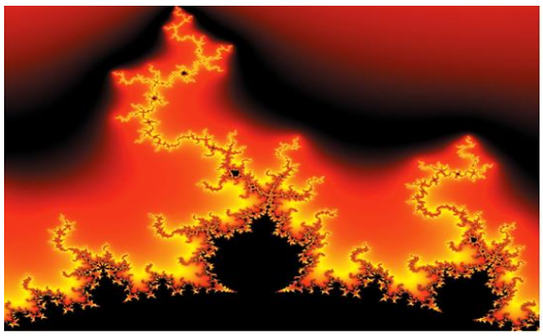

Figure 1 Title and *Source (in italics)*

Should not be images-everything must be editable.

Table 1 Title and *Source (in italics)*

Should not be images-everything must be editable.

Each article shall present separately in **3 folders**: a) Figures, b) Charts and c) Tables in .JPG format, indicating the number and sequential Bold Title.

For the use of equations, noted as follows:

$$Y_{ij} = \alpha + \sum_{h=1}^{r} \beta_h X_{hij} + u_j + e_{ij} \qquad (1)$$

Must be editable and number aligned on the right side.

Methodology

Develop give the meaning of the variables in linear writing and important is the comparison of the used criteria.

Results

The results shall be by section of the article.

Annexes

Tables and adequate sources thanks to indicate if were funded by any institution, University or company.

ISSN: 2410-4191

Conclusions

Explain clearly the results and possibilities of improvement.

References

Use APA system. Should not be numbered, nor with bullets, however if necessary numbering will be because reference or mention is made somewhere in the Article.

Use Roman Alphabet, all references you have used must be in the Roman Alphabet, even if you have quoted an Article, book in any of the official languages of the United Nations (English, French, German, Chinese, Russian, Portuguese, Italian, Spanish, Arabic), you must write the reference in Roman script and not in any of the official languages.

Technical Specifications

Each article must submit your dates into a Word document (.docx):

Journal Name
Article title
Abstract
Keywords
Article sections, for example:

1. Introduction
2. Description of the method
3. Analysis from the regression demand curve
4. Results
5. Thanks
6. Conclusions
7. References

Author Name (s)
Email Correspondence to Author
References

Intellectual Property Requirements for editing:

-Authentic Signature in Color of Originality Format Author and Coauthors

-Authentic Signature in Color of the Acceptance Format of Author and Coauthors

ISSN: 2410-4191

Reservation to Editorial Policy

ECORFAN-Journal Bolivia reserves the right to make editorial changes required to adapt the Articles to the Editorial Policy of the Journal. Once the Article is accepted in its final version, the Journal will send the author the proofs for review. ECORFAN® will only accept the correction of errata and errors or omissions arising from the editing process of the Journal, reserving in full the copyrights and content dissemination. No deletions, substitutions or additions that alter the formation of the Article will be accepted.

Code of Ethics - Good Practices and Declaration of Solution to Editorial Conflicts

Declaration of Originality and unpublished character of the Article, of Authors, on the obtaining of data and interpretation of results, Acknowledgments, Conflict of interests, Assignment of rights and Distribution.

The ECORFAN-Mexico, S.C Management claims to Authors of Articles that its content must be original, unpublished and of Scientific, Technological and Innovation content to be submitted for evaluation.

The Authors signing the Article must be the same that have contributed to its conception, realization and development, as well as obtaining the data, interpreting the results, drafting and reviewing it. The Corresponding Author of the proposed Article will request the form that follows.

Article title:

- The sending of an Article to ECORFAN -Journal Bolivia emanates the commitment of the author not to submit it simultaneously to the consideration of other series publications for it must complement the Format of Originality for its Article, unless it is rejected by the Arbitration Committee, it may be withdrawn.

- None of the data presented in this article has been plagiarized or invented. The original data are clearly distinguished from those already published. And it is known of the test in PLAGSCAN if a level of plagiarism is detected Positive will not proceed to arbitrate.

- References are cited on which the information contained in the Article is based, as well as theories and data from other previously published Articles.

- The authors sign the Format of Authorization for their Article to be disseminated by means that ECORFAN-Mexico, S.C. In its Holding Bolivia considers pertinent for disclosure and diffusion of its Article its Rights of Work.

- Consent has been obtained from those who have contributed unpublished data obtained through verbal or written communication, and such communication and Authorship are adequately identified.

- The Author and Co-Authors who sign this work have participated in its planning, design and execution, as well as in the interpretation of the results. They also critically reviewed the paper, approved its final version and agreed with its publication.

- No signature responsible for the work has been omitted and the criteria of Scientific Authorization are satisfied.

- The results of this Article have been interpreted objectively. Any results contrary to the point of view of those who sign are exposed and discussed in the Article.

Copyright and Access

The publication of this Article supposes the transfer of the copyright to ECORFAN-Mexico, SC in its Holding Bolivia for its ECORFAN -Journal Bolivia, which reserves the right to distribute on the Web the published version of the Article and the making available of the Article in This format supposes for its Authors the fulfilment of what is established in the Law of Science and Technology of the United Mexican States, regarding the obligation to allow access to the results of Scientific Research.

Article Title:

Name and Surnames of the Contact Author and the Coauthors	Signature
1.	
2.	
3.	
4.	

Principles of Ethics and Declaration of Solution to Editorial Conflicts

Editor Responsibilities

The Publisher undertakes to guarantee the confidentiality of the evaluation process, it may not disclose to the Arbitrators the identity of the Authors, nor may it reveal the identity of the Arbitrators at any time.

The Editor assumes the responsibility to properly inform the Author of the stage of the editorial process in which the text is sent, as well as the resolutions of Double-Blind Review.

The Editor should evaluate manuscripts and their intellectual content without distinction of race, gender, sexual orientation, religious beliefs, ethnicity, nationality, or the political philosophy of the Authors.

The Editor and his editing team of ECORFAN® Holdings will not disclose any information about Articles submitted to anyone other than the corresponding Author.

The Editor should make fair and impartial decisions and ensure a fair Double-Blind Review.

Responsibilities of the Editorial Board

The description of the peer review processes is made known by the Editorial Board in order that the Authors know what the evaluation criteria are and will always be willing to justify any controversy in the evaluation process. In case of Plagiarism Detection to the Article the Committee notifies the Authors for Violation to the Right of Scientific, Technological and Innovation Authorization.

Responsibilities of the Arbitration Committee

The Arbitrators undertake to notify about any unethical conduct by the Authors and to indicate all the information that may be reason to reject the publication of the Articles. In addition, they must undertake to keep confidential information related to the Articles they evaluate.

Any manuscript received for your arbitration must be treated as confidential, should not be displayed or discussed with other experts, except with the permission of the Editor.

The Arbitrators must be conducted objectively, any personal criticism of the Author is inappropriate.

The Arbitrators must express their points of view with clarity and with valid arguments that contribute to the Scientific, Technological and Innovation of the Author.

The Arbitrators should not evaluate manuscripts in which they have conflicts of interest and have been notified to the Editor before submitting the Article for Double-Blind Review.

Responsibilities of the Authors

Authors must guarantee that their articles are the product of their original work and that the data has been obtained ethically.

Authors must ensure that they have not been previously published or that they are not considered in another serial publication.

Authors must strictly follow the rules for the publication of Defined Articles by the Editorial Board.

The authors have requested that the text in all its forms be an unethical editorial behavior and is unacceptable, consequently, any manuscript that incurs in plagiarism is eliminated and not considered for publication.

Authors should cite publications that have been influential in the nature of the Article submitted to arbitration.

Information services

Indexation - Bases and Repositories

LATINDEX (Scientific Journals of Latin America, Spain and Portugal)
RESEARCH GATE (Germany)
GOOGLE SCHOLAR (Citation indices-Google)
REDIB (Ibero-American Network of Innovation and Scientific Knowledge- CSIC)
MENDELEY (Bibliographic References Manager)

Publishing Services:

Citation and Index Identification H.
Management of Originality Format and Authorization.
Testing Article with PLAGSCAN.
Article Evaluation.
Certificate of Double-Blind Review.
Article Edition.
Web layout.
Indexing and Repository
ArticleTranslation.
Article Publication.
Certificate of Article.
Service Billing.

APC regulations

The APC Publication Rate must only be made by the corresponding author, with the understanding that the Coauthors are third parties who supported the development of the article and these are included in the same rate, with the same rights and privileges of the work, as noted In the principles of Ethics and Conduct of ECORFAN-Mexico, SC, supporting those who have less access to information and those emanated from the International Service of Science and Technology of the IDB, WIPO, OAS, OECD and UN.

Editorial Policy and Management

244 – 2 Itzopan Street La Florida, Ecatepec Municipality Mexico State, 55120 Zipcode, MX. Phones: +52 1 55 2024 3918, +52 1 55 6159 2296, +52 1 55 4640 1298; Email: contact@ecorfan.org www.ecorfan.org

ECORFAN Journal-Bolivia

2410 4191
ISSN 2410 - 4191

www.ecorfan.org